ADVANCED MATERIALS
www.advmat.de

Transparent Soft Actuators/Sensors and Camouflage Skins for Imperceptible Soft Robotics

*Phillip Won, Kyun Kyu Kim, Hyeonseok Kim, Jung Jae Park, Inho Ha, Jaeho Shin, Jinwook Jung, Hyunmin Cho, Jinhyeong Kwon, Habeom Lee, and Seung Hwan Ko**

The advent of soft robotics has led to great advancements in robots, wearables, and even manufacturing processes by employing entirely soft-bodied systems that interact safely with any random surfaces while providing great mechanical compliance. Moreover, recent developments in soft robotics involve advances in transparent soft actuators and sensors that have made it possible to construct robots that can function in a visually and mechanically unobstructed manner, assisting the operations of robots and creating more applications in various fields. In this aspect, imperceptible soft robotics that mainly consist of optically transparent imperceptible hardware components is expected to constitute a new research focus in the forthcoming era of soft robotics. Here, the recent progress regarding extended imperceptible soft robotics is provided, including imperceptible transparent soft robotics (transparent soft actuators/sensors) and imperceptible nontransparent camouflage skins. Their principles, materials selections, and working mechanisms are discussed so that key challenges and perspectives in imperceptible soft robotic systems can be explored.

1. Introduction

Over the decades, robots with rigid connected parts have far been researched to assist the fields of military services, surgical instruments, and wearable assistive devices, but which mostly are restricted to discrete motions. However, soft robotics with entirely soft bodied system often solve difficulties in conventional rigid robots by overcoming their constraints, exceeding the performances and creating new applications.[1–3] Therefore, these soft machines have already taken many roles in industrial processing, automation, marine engineering, etc.[4–6]

Technological advances in robots and wearable devices are closely connected to optical and mechanical compliance depending on their use. By taking advantages of recent advancements in transparent actuators and sensors, combining their soft and stretchy mechanical compliance with optically transparent property affords to create a new class of soft robotics, which can be referred to as an imperceptible soft robotics (ISR). As shown in **Figure 1**, systematic diagram of imperceptible soft robotics describes that ISR will mainly consist of transparent systems and camouflage skin. Transparent systems embrace optically transparent soft actuators and sensors in order to build mechanically interactive robotics that are rarely seen by others. As a supportive component, camouflage skin aims to provide for transparent systems to adapt in natural environment or humans for undercover operation and safe user-friendly interactions. This new conception of imperceptible soft robotic system that exhibits optically transparent interface or visually imperceptions through camouflage skin provides new functionalities over ones without such properties. Imperceptions of an assistive wearable device can be crucially important in wearer's daily life. Mechanically compliant and visually imperceptive human assistive device can serve the user's rehabilitation process or support disabled parts in the body without discomfort, altering biomechanics, and obstructive to others.[7] In a similar fashion, robotic prosthetics that requires soft sensing capability of motherly touch for caring babies demand integrated sensors and actuators to be imperceptible.[8] Tactile sensation with an implementation of ISR delivering information to user in private also possesses a wide range of possibility in virtual/augmented reality for human–machine interface and smart-living environment.[9–12] Undercover mission enabled by disguising into nature through optical transparency or environmentally skin will also be achieved by imperceptible

P. Won, K. K. Kim, H. Kim, J. J. Park, I. Ha, Dr. J. Shin, Dr. J. Jung, Dr. H. Cho, Prof. S. H. Ko
Applied Nano and Thermal Science Lab
Department of Mechanical Engineering
Seoul National University
1 Gwanak-ro, Gwanak-gu, Seoul 08826, South Korea
E-mail: maxko@snu.ac.kr

Dr. J. Kwon
Manufacturing System R&D Group
Korea Institute of Industrial Technology (KITECH)
89 Yangdaegiro-gil, Ipjang-myon, Seobuk-gu, Cheonan, Chungcheongnam-do 31056, South Korea

Prof. H. Lee
School of Mechanical Engineering
Pusan National University
2 Busandaehag-ro, 63 Beon-gil, Geumjeong-gu, Busan 46241, South Korea

Prof S. H. Ko
Institute of Advanced Machines and Design/Institute of Engineering Research
Seoul National University
Seoul 08826, South Korea

The ORCID identification number(s) for the author(s) of this article can be found under https://doi.org/10.1002/adma.202002397.

DOI: 10.1002/adma.202002397

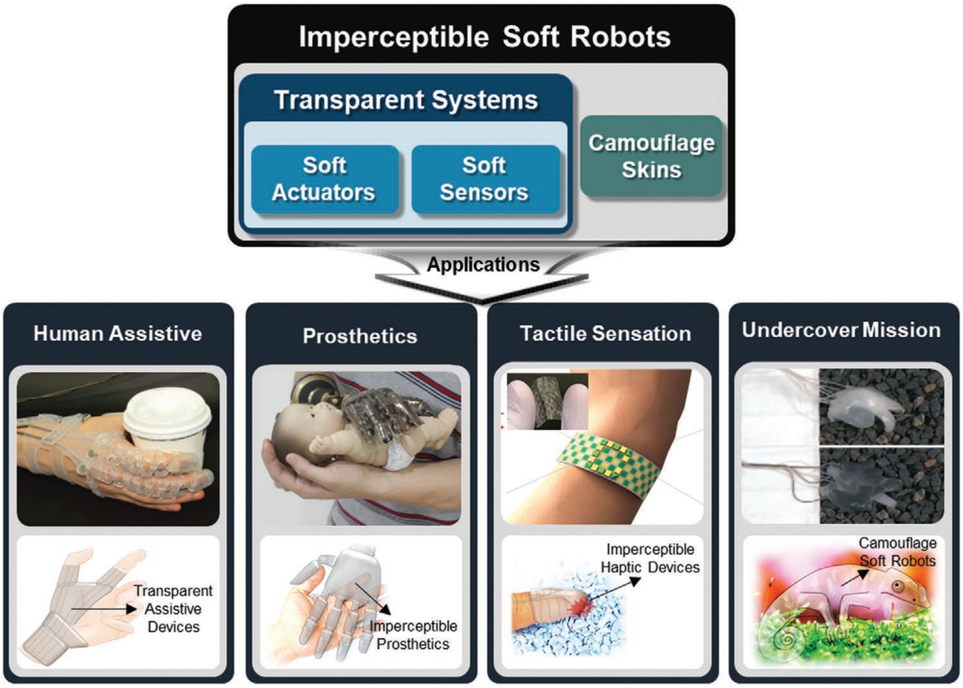

Figure 1. Systematic diagram of imperceptible soft robotics (ISR). Various potential applications in robotic fields for ISR: a human-assistive device, robotic prosthetics, and a soft undercover robot. Soft exo-glove image: Reproduced with permission.[132] Copyright 2019, Mary Ann Liebert, Inc. Image of skin-like soft electronics for prosthetics. Reproduced with permission.[144] Copyright 2014, Springer Nature. Image of transparent piezoelectric actuator/sensor patch for human–machine interaction. Reproduced with permission.[145] Copyright 2019, American Chemical Society. Image of soft machines camouflaged by injection of pigments. Reproduced with permission.[13] Copyright 2012, AAAS.

soft robotics for military applications.[13] The concept of imperceptible soft robotics is learned from living organisms by understanding the ultimate goals of the unique optical function and adapting the capability given to them in similar ways.[13–15] Our conceptual inspiration derived from how a chameleon protects himself from predators with camouflage skin and able to produce locomotion while hardly perceptive by others similar to the expression by a cartoon in **Figure 2**. In this progress report, we are going to cover the advancements of imperceptible soft robotics into three distinctive parts: three main components for hardware in imperceptible robotic system—1) transparent soft actuators, 2) transparent soft sensors, and 3) camouflage skin.

First, recent advancements in transparent soft actuators will be introduced respect to actuation mechanisms. The transparent soft actuators, addressed by far, exploit basically the same working mechanisms regardless of its transparent body, including pneumatic/hydraulic inflation, dielectric elastomers actuation, electrothermal actuation, and various stimulus responsive actuations.[6,16–19] The actuators can be employed as physically interactive surfaces, transparent muscles, and untethered robots that work in insensible or imperceptible manner in variety of applications. However, their current challenges such as actuation force, power consumption, and spatial resolution of actuation area must be solved to utilize as transparent muscles in imperceptible soft robotics.[17,18,20] In this regard, we will also discuss about challenges of recent transparent soft actuators from each reports and guide with possible solutions for further development.

Next, two main categories of transparent soft sensors will be presented to discuss their recent developments: 1) patterning enabled transparent sensor and 2) intrinsically transparent sensor. Strategies to fabricate the transparent soft sensors may vary critically with materials. Transparency and softness of the sensor can be given by various fabrication strategies using open-mesh structure and wavy pattern although the materials' intrinsic property is stiff and bulky. On the other hand, intrinsically soft and transparent property of various kinds of materials can be easily integrated into transparent soft sensors. In the field of flexible/stretchable electronics, typically sensor parts, researchers have made their persistent efforts to improve the versatility of skin-like soft sensors in health-monitoring, human–machine interactions, and robotic perceptions.[21–24] Sensors that are unseen or unnoticeable to both users and others often give routes to transmit external stimuli to users in private. Since physical properties of such sensors making easy to implement into other surfaces such as robots, human skin, next generation of applications aside from health monitoring. Based on this movement, their current interests lie in integration of prevalently developed soft skin-like sensors to soft compliant actuators.[22] Therefore, there will be a synergistic merging in the two research fields by taking complementary aspects so that this approach can in turn constitute a new innovation in the soft robotics field.

Moreover, as a skin part that retains additional element in imperceptible soft robotics, camouflage system can be a great alternative to optically transparent materials. Utilizing environmentally adaptive artificial skin of the soft robot enables to

Figure 2. Compositions of imperceptible soft robotics (ISR). Three distinctive categories that comprise imperceptible soft robotics—transparent soft actuators, transparent soft sensors, and camouflage skins. Initial inspiration came from functionalities that chameleons utilize in response to their environment. The rapid development in such optically functional actuators, sensors, and skins would enable imperceptible soft robotics by merging listed examples together. Transparent Actuators. Image for "Functional composite": Reproduced with permission.[19] Copyright 2015, Springer Nature. Image for "ETAs": Reproduced with permission.[17] Copyright 2019, Mary Ann Liebert, Inc. Image for "DEAs": Reproduced with permission.[4] Copyright 2018, The Authors, published by AAAS. Image for "Hydraulic": Reproduced under the terms of the CC-BY Creative Commons Attribution 4.0 Internation license (https://creativecommons.org/licenses/by/4.0).[65] Copyright 2017, The Authors, published by Springer Nature. Image for "SMP": Reproduced with permission.[70] Copyright 2013, Wiley-VCH. Soft sensors. Image for "Ultrathin electronics": Reproduced with permission.[86] Copyright 2016, Wiley-VCH. Image for "Electronic Tattoo": Reproduced with permission.[81a] Copyright 2017, American Chemical Society. Image for "Ionic skin": Reproduced with permission.[82] Copyright 2016, AAAS. Image for "Microfluidic elastomer": Reproduced with permission.[99] Copyright 2011, IEEE. Image for "Percolation network": Reproduced with permission.[115] Copyright 2018, Wiley-VCH. Camouflage Skins. Image for "Shape morphing": Reproduced with permission.[25] Copyright 2017, The Authors, published by AAAS. Image for "Color shifting": Reproduced with permission.[130] Copyright 2018, Wiley-VCH. Image for "Opacity switching": Reproduced with permission.[123] Copyright 2020, Wiley-VCH.

conceal itself within their surrounding environments by adjusting their skin color, opacity, and reshaping morphology.[13,25]

Extended study on integrated system of sensors and actuators existing as subsystems to fully track down motions and trajectories of soft body currently attract many interests to allow better control of the system. Moreover, the development of untethered operation and advanced sensory system enables further enhancement of the soft robotic system.

Key advancements and properties in transparent soft actuators, sensors and camouflage skins for designing imperceptible soft robotics are organized in Figure 2. Convergence in these technologies has brought us to develop imperceptible soft robotics for various new applications. Hence, we will be also dealing with the perspectives on three distinctive components will be thoroughly considered for more advanced and applicable imperceptible soft robotics in this progress report.

2. Transparent Soft Actuators

For robots to move and interact freely with environments, their robotic body requires actuation system that generates various motions. Soft actuators, as the word, "soft" intuitively refers, must have soft body that are reliably compliant to any surfaces unlike conventional bulky and rigid bodied actuators.[26–28] Since soft actuators are endowed with many potentials in robotic field, there are a number of efforts to bring out the performance that completely alters the current robotic system. Therefore, representative progress on soft actuation systems often involves hydraulically or pneumatically powered actuators with soft channeled system, external stimuli-responsive actuators, etc.[29–31] Besides the general idea to develop the soft actuators, the ability to disguise and to adapt in environment in soft robotics arises as a great interest with a need for undercover missions and assistive wearable devices, where unobstructed operations should take places. Generally, soft actuators with transparent materials show optical transparency for the entire system. Previous studies on various soft actuators, such as dielectric elastomer actuators (DEAs) and electrothermal actuators (ETAs) using transparent materials, have shown the possibility of developing the latest transparent actuators. In addition, development of advanced materials such as functional polymers and hydrogels that respond to various external stimuli such as heat, light, and pH[26,32–35] broadens the possibilities of alternative mechanisms and various practical applications for soft actuators. Examples of transparent soft actuators are briefly described in **Table 1** by actuation types and stimulus,

Table 1. Transparent soft actuators.

Actuation types	Stimulus	Actuation force [mN]	Actuation speed [Hz]	Strain [%]	Maximum curvature [cm^{-1}]	Energy efficiency [%]	Power output [mW]	Size [mm]	Weight [mg]	Transparency [%]	Material	Ref.
ETAs	DC 1–3 V	3920	0.004	41	–	–	–	15 × 26	1×10^3	–	Liquid crystal elastomer	[39]
	DC 15 V	0.29	0.1	–	2.6	33.8	–	10 × 30	12.7	80	LDPE, PVC, AgNW	[17]
	DC 120 V	–	0.003	–	1	–	–	47 × 10	–	83	Paraffin wax, PDMS, PET, SACNT	[44]
	DC 5 V	–	0.006	–	1.12	–	–	–	–	82	PDMS, AgNW	[147]
	DC 5–30 V	0.32	5	–	2.3	–	–	3 × 10	2.7	–	PDMS, PEDOT:PSS	[148]
	DC 5.1 V	43.4	0.07	0.15	0.29	–	0.44	35 × 10	48	–	MXene ($Ti_3C_2T_x$), cellulose	[149]
DEAs	DC 12 kV	550	126	118	–	19.4	0.345	980 × 220	2.3×10^3	–	Liquid dielectric, PAM hydrogel, BOPP	[62]
	DC 7.5–10 kV	0.25	0.33–0.5	–	0.125	0.0013	0.08×10^{-3}	220 × 50	–	94	VHB tape, water	[4]
	AC 7–10 kV (5–8 Hz)	6–18	5–8	2–4	–	10	2.43	2200 × 930	90.3×10^3	–	VHB tape, hydrogel, acrylonitrile butadiene styrene	[64]
	AC 10 kV (10 Hz)	–	5–20	200	0.003	–	–	260 × 75	–	90	VHB tape, PEDOT: PSS/WPU, PET	[15]
	DC 0.5–1.5 kV	686	0.5	16–23	–	0.164	0.258	20 × 15	70×10^3	–	PVC gel, graphene oxide	[52]
	AC 3.3 kV (20 Hz)	–	20	140	–	–	–	45 × 7	–	96.95	VHB tape, poly(acrylic acid) ionogel	[16]
	AC 0–18 kV (0.05–1024 Hz)	–	$20–20 \times 10^3$	167	–	–	–	40 × 40	–	–	VHB tape, PAM hydrogel	[18]
	DC 6 kV	–	–	146	–	–	–	15 × 15	–	–	VHB tape, AgNW/CNT	[58]
Alternative actuations	Hydraulic force	≈10 000	≈1	≈300	–	–	–	130 × 90	–	95	Tough hydrogels, water	[65]
	Temperature (>50 °C)	6.13	0.01	≈50	–	–	–	40 × 4	–	–	rbSME	[70]
	Temperature (>23 °C)	40	0.006	–	0.5	–	–	25 × 2	40	–	Liquid crystal elastomer network	[71]
	Ion triggered shape memory effect ($ZnCl_2$)	–	0.2	≈200	–	–	–	50 × 2	–	–	Poly(acrylonitrile 2-methacryloyloxyethyl phosphoryl-choline) copolymer hydrogels	[150]
	Temperature (>32 °C)	180	0.5	170	–	–	–	10 × 10	–	–	PNIPA/TiNSs	[19]
	Infrared-light	0.2	1	–	4.7	–	0.0018	3 × 6		80	PE, graphene	[68]
	Temperature (>50 °C)	–	6×10^{-4}	10	–	–	–	5.5 × 5.5	–	–	P(OEGMA-DSDMA), poly(acrylamide-*N*,*N*′-bis (acyloyl)cystamine) hydrogel	[67]

materials and characteristics. Beyond progress of aforementioned research, we will discuss perspectives in transparent soft actuators respect to their actuation types.

2.1. Transparent Soft Actuators: ETAs

Heat, which is a primitive energy source over a long period of time, has been an effective actuation stimulus in recent advances of soft robotics. Since the heat delivered within actuators is not visible to eyes, transparent ETAs may be considered a very intuitive and practical way to an imperceptible actuating system. Generally, the ETAs employ resistive heating induced by applying current through electrodes for supplying thermal energy to the surfaces in contact with electrodes. Though there have been a number of ETAs using smart materials like shape-memory alloys (SMAs) to generate motions through transition in their crystallinity,[36] many candidates are excluded from the materials choices due to their inability to function in visually transparent manner. As a consequence, many transparent soft ETAs that will be summarized below often possess transparent heater and transparent thermoresponsive layers, bringing soft actuators closer to optically invisible functionality. In this regard, most transparent ETAs will utilize the large thermal expansion of materials to induce shrinkage or expansion of single or multiple thin-film layers.

To enhance actuation range of ETA, a thermoresponsive liquid crystal elastomer (LCE) has been shown recently with distinctive properties by the rearrangement of liquid crystals within the elastomer.[37,38] As the temperature of the LCE increases, the transition of liquid crystal mesogen from nematic phase to isotropic phase induces macroscopic deformation of the system. These features enable large deformation during the actuation and overcome the limitations of the conventional light weight ETAs, which have low actuation force. **Figure 3**a displays a transparent LCE-based actuator that is composed of a thin stretchable serpentine resistive heater inserted in between two layers of loosely crosslinked LCE films to establish an ETA-based artificial muscle.[39] With more shrinkable characteristic of LCE film compared to other ETA, the artificial muscle can be contracted 41% of its initial length and generate high actuation stress over 0.35 MPa upon resistive heating with 3.0 V applied voltage. In addition, the LCE artificial muscle can also lift a load of 400 g by dissipating 38% actuation strain (Figure 3a, bottom). The LCE tubular actuator aligned with the three individually controlled heaters can generate vertical contraction and directional bending, enabling multimodal actuation similar to human muscles.

Most generalized form of ETA is a bilayer actuator that exploits bilayering two transparent polymer films with different thermal expansion coefficients.[40,41] By virtue of its simple structure and easy fabrication procedure, a bilayered ETA not only offers much more simplicity in design and versatility but also provides meaningful aspects over other soft actuator. Such ETAs usually exhibit large bending actuations, even with relatively small film thickness, expansions, and low energy consumption.[42,43] Our group has also sought to develop a bilayer ETA, which we refer as an anisotropic transparent shape morphing (ATSM) actuator.[17] The ATSM uses silver nanowires (AgNWs) percolation network heater placed in between isotropic and anisotropic polymer films to derive thermal actuation in a machine direction of anisotropic polymer film (LDPE: low-density polyethylene). Figure 3b shows the ATSM actuator capable of inducing large deformation (curvature > 2.5 cm^{-1}) at modest temperature condition (40 °C). Using

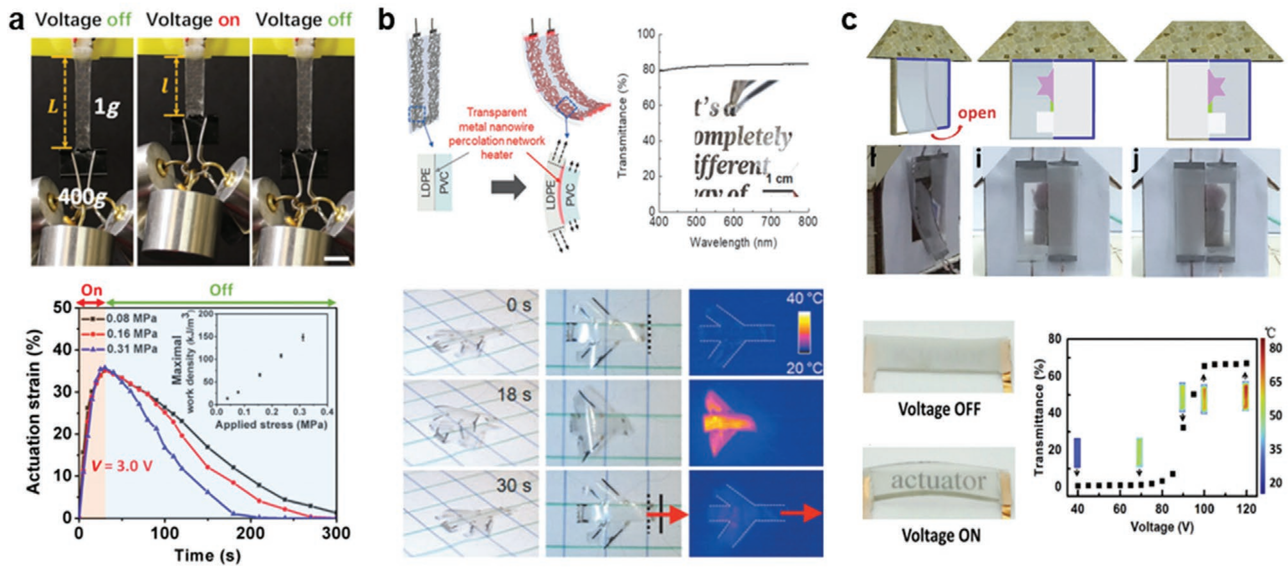

Figure 3. Transparent electrothermal actuators (ETAs). a) Thermoresponsive liquid crystal elastomer (LCE) based artificial muscle film with a reversible actuation and thermomechanical property. Reproduced with permission.[39] Copyright 2019, The Authors, published by AAAS. Reprinted/adapted from ref. [39]. © The Authors, some rights reserved; exclusive licensee American Association for the Advancement of Science. Distributed under a Creative Commons Attribution NonCommercial License 4.0 (CC BY-NC) http://creativecommons.org/licenses/by-nc/4.0/. b) Bilayered transparent actuator integrated with NWs heater and anisotropic polymer film and transparent walking robot in IR images respect to DC images for visualization of movement. Reproduced with permission.[17] Copyright 2019, Mary Ann Liebert, Inc. c) Transparency-switchable actuator using PW-PDMS/SACNT composite and its switchable optical transparency at distinctive temperature regime by applied voltages. Reproduced with permission.[44] Copyright 2017, Elsevier.

the simple structural advantage of the ATSM, the transparent ATSM is designed into the transparent walking robot to show directional controllability in real-time stimulated by thermal actuations (Figure 3b).

Since heat is also a source of stimuli for other functionality, the work by Zhang et al. introduced a heat-induced optically switchable soft body that can also make bending motion simultaneously.[44] This multifunctional ETA incorporates a single-layer superaligned carbon nanotube (SACNT) transparent heater, and a poly(dimethylsiloxane) (PDMS) layer as a backbone heater electrode layer in order to construct a bilayer actuating system with large difference in their coefficients of thermal expansion (CTEs of PDMS and SACNT: 310 and 6 ppm K^{-1}, respectively). A mixture of PDMS and paraffin wax (PW) is the optically switchable layer coated on top of the electrode. Hardening/melting of paraffin wax droplets in the mixture changes the degree of light scattering at distinctive temperatures. Hence, the ETA made of PW-PDMS/SACNT offers optical switching capability from the opaque (<55 °C) to transparent (>55 °C) with bending actuation (Figure 2f). As a proof of concept, the PW-PDMS/SACNT actuator has been demonstrated as a smart window (Figure 2c). Thus, this transparent soft actuator can potentially be employed as on-demand transparency-switchable robotic skin and muscle for imperceptible soft robotics.

Transparent ETAs can show bending motions by utilizing large coefficient of thermal expansion. ETAs have advantages of low energy consumption and can be quantitatively controlled by manipulating input electricity unlike the other actuators driven by light or pH. However, the lightweight thin film structured nature of ETA is a big limiting factor that can be challenged by other bulky soft actuators with stronger output force. Since the actuation is mainly dependent on the rate of heating and cooling, integration of rapid temperature transition system such as thermally conductive element will greatly influence the system's performance.

2.2. Transparent Soft Actuators: DEAs

Another representative class of a transparent soft actuator is a DEA.[45] DEA is an actuator that uses a high-voltage driven strong electric field to deform a dielectric material sandwiched between two complaint electrodes.[46] In previous works on DEAs, the compliant electrodes that were usually made of carbon powder or carbon grease did not exhibit optical transparency and high mechanical durability.[47–49] However, in recent advances in transparent soft actuators, DEAs are taking most places that guarantee forementioned limiting factors: reliable mechanical property and optical transparency, as the development of transparent compliant electrodes, including ionic conductive hydrogels,[50–52] graphene,[53,54] carbon nanotubes (CNTs),[55–57] and metal nanowire,[58,59] continues to advance.

DEAs typically show fast actuation speed, large strains, and high forces generation,[16,60,61] the recent work by Keplinger and co-workers has made use of these properties in hydraulically amplified self-healing electrostatic (HASEL) actuator that achieve fast actuation with a zipping mechanism (**Figure 4**a).[62] The HASEL actuator is easily fabricated by injection of polyacrylamide (PAM) hydrogel into the channels that are formed

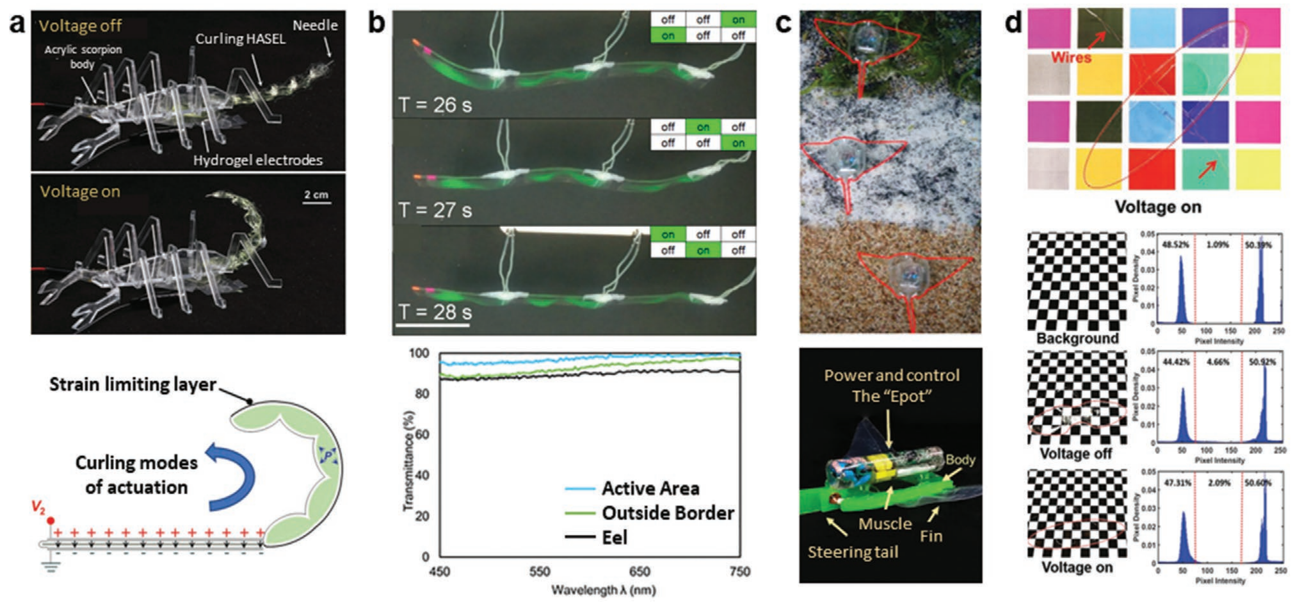

Figure 4. Transparent dielectric elastomer actuators (DEAs). a) Hydraulically amplified self-healing electrostatic (HASEL) actuator in a scorpion robot and description of a zipping driven DEA using liquid dielectric materials. Reproduced under the terms of the CC-BY Creative Commons Attribution 4.0 International license (https://creativecommons.org/licenses/by/4.0).[62] Copyright 2019, The Authors, published by Wiley-VCH. b) Fluid electrode dielectric elastomer actuator (FEDEA) mimicking a transparent eel and comparison of the optical transparency between the FEDEA and the eel (leptocephalus). Reproduced with permission.[4] Copyright 2018, The Authors, published by AAAS. c) Electroionic fish with all transparent layers and onboard system for power and remote control. Reproduced with permission.[64] Copyright 2017, The Authors, published by AAAS. Reprinted/adapted from ref. [64]. © The Authors, some rights reserved; exclusive licensee American Association for the Advancement of Science. Distributed under a Creative Commons Attribution NonCommercial License 4.0 (CC BY-NC) http://creativecommons.org/licenses/by-nc/4.0/. d) Transparent soft robot with biaxially prestretched membranes and light scattering-free surface under actuation. Reproduced with permission.[15] Copyright 2019, Wiley-VCH.

by thermally zipping two thermoplastic films. The HASEL actuator shows remarkable actuation performances, providing strain generations up to 118%, strain rates of about 7500% s^{-1}, actuation frequency of 126 Hz, and specific power of 156 W kg^{-1}. The shape of HASEL actuator can be easily designed into a scorpion's tail (Figure 4a, bottom) that resembles the same high-speed stroke of an actual scorpion tail with rapid actuation speed of 1.26 m s^{-1} upon its full curling.

Among the living creatures, many organisms such as the eel, squid, octopus, surgeonfish, and butterfly have camouflage body that is similar to optical property of their living environment to disguise themselves from predators.[63] By mimicking the camouflage capability of these organism, Christianson et al. have introduced a fluid electrode DEA (FEDEA) that disguises underwater because of watery body with the same refractive index and bimorphs to take swimming motions similar to the locomotion of the transparent eel, leptocephalim (Figure 4b).[4] The typical eel-like FEDEA configures into three aligned DEAs that each bimorph and separately actuate on-demand by taking the aquatic environment as an electrical ground. Furthermore, the optical transparency of the FEDEA with the actuator and border parts has shown a comparable high transmittance above 90% in the water which is also similar to the eel across all visible spectra (Figure 4b, bottom).

In addition to the camouflage ability underwater, the research on the transparent DEA with untethered system has been studied by Li et al.[64] Motivated by manta-ray's structure and its propulsion mechanism, an electroionic fish is designed in all transparent parts where elastomeric body frame guides a prestretched hydrogel layer to naturally deform into manta-ray-like configuration (Figure 4c). In addition, the integration of electronic pod (Epod) (Figure 4c, bottom) to the propelling body replaces wired power source with built in high-voltage amplifier, lithium-ion battery, and infrared (IR) remote control circuits with comparably lightweights. Such compact electronic system can operate the electroionic fish at fast swimming speed of 0.69 body length s^{-1} with boosted applied voltage in completely untethered mode. However, the speed of untethered mode significantly decreases in half as the weight of ionic fish doubles with the Epod.

Another transparent dielectric actuator proposed by Li et al. (Figure 4d) employs transparent and stretchable conductive polymers blends of poly(3,4-ethylenedioxythiophene): poly(styrenesulfonate) (PEDOT:PSS) and water-borne polyurethane (WPU) as compliant solid-state electrodes in the DEAs.[15] This conductive polymer based DEA shows large voltage-induced area up to strain of 200% and a high transmittance of 85.5%. The prestretched elastic layer interacting with another elastic body enables to form 3D twisted robotic body that reacts to the DC voltage to become completely 2D flat structure in simple and fast way. When the voltage is on, the conductive polymer DEA perfectly flattens out the entire surface and camouflages into various colored (or black/white) backgrounds by minimized light reflection. (Figure 4d, bottom).

Most of examples in transparent DEAs can still exhibit the advantages like fast actuation speed and high force generation while maintaining transparent and imperceptible characteristics. Competitiveness in actuation performance among soft actuation systems makes DEAs plausible candidate in imperceptible soft robotics. Prerequisites for DEA such as high voltage and external circuit require the hardware that limits the actuation system from operating in untethered form. However, as the recent work shown its potential with their wireless-power system, there may be further development in energy storage devices to operate the actuation with higher output forces or to supply in transparent platform, contributing to achieve fully imperceptible untethered robotics.

2.3. Transparent Soft Actuators: Alternative Actuations

Apart from DEA, ETAs, there still exist other types of transparent soft actuators with alternative actuations such as pneumatic/hydraulic actuators,[65,66] and functional composite actuators.[19,67–71] Although pneumatic soft actuators generally require an external source of compressed air applied by the valve system, they have advantages of high output force and maintain their shapes without additional input energy.[72] Soft actuators made of functional composites usually do not rely on electrical powers instead utilize environmental stimuli such as humidity, pH, and surrounding temperature.[73,74]

Aside from pneumatically powered actuator, hydraulic-driven actuators are introduced by Yuk et al.[65] Transparent robust hydrogel skins as the hydraulic chamber sustain over 1000 cycles of hydraulic pressure-driven actuations without leakage or failure. Since the hydraulic chamber is comprised mostly with water, the presented actuator embodies almost the same optical and sonic properties in water, making the whole system disappear from an aquatic environment (**Figure 5**a). With this camouflage feature, a transparent robotic fish, a finger, and a gripper are demonstrated to show an advantage of imperceptible motions (Figure 5a, bottom). As a result, hydraulic actuator composed of tough hydrogel has proven to show the highest output force (10 N) among any other transparent soft actuator.

Shape memory polymers (SMPs) are functional materials that can reconfigure their shape under certain temperatures.[75] To overcome the irreversibility of common SMPs, one research group has presented reversible, bidirectional shape-memory effect (rbSME) to manipulate a transparent gripper in grasping/releasing modes by controlling the surrounding temperature.[70] The rbSME comprises two domains, in which one that determines the skeleton and the other that acts to a thermal stimulus. The transparent gripper that shows the rbSME is therefore programmable at higher temperature and repeatedly actuated in response to cooling and heating (Figure 5b). Moreover, 3D printing of hydrogel in a high resolution (micrometer scale) while maintaining the merits of hydrogel stretchability, toughness, and resilience and ionically conductive has been demonstrated by Giannelis's group (Figure 5c).[76] Along with their notable mechanical properties, this hydrogel exhibits fast photopolymerization to allow rapid 3D printing. Both 3D printed cubic lattice and multiarmed gripper are fabricated to display their fast swelling capabilities (Figure 5c, bottom).

From a group in Japan, Kim and co-workers have designed an actuator consisting of multilayered with structure cofacially oriented titanate nanosheets (TiNSs) and poly(*N*-isopropylacrylamide) (PNIPA) to generate faster and stronger actuation than single component responsive device.[19] Addition of PNIPA in the composite changes electrostatic permittivity near 32° because

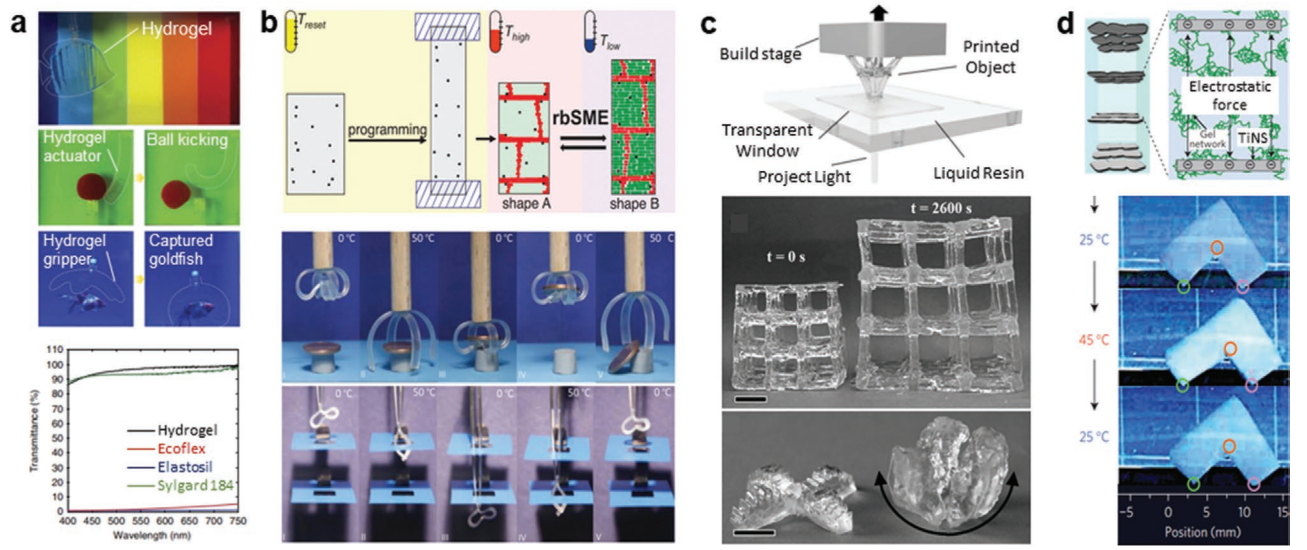

Figure 5. Alternative actuation types in transparent soft actuators. a) Hydraulically powered actuators and their optical properties. A transparent robotic fish, a finger, and a gripper that are mainly made of hydrogels are camouflaged in an aquatic environment to demonstrate an advantage of imperceptible motions. Reproduced under the terms of the CC-BY Creative Commons Attribution 4.0 International license (https://creativecommons.org/licenses/by/4.0).[65] Copyright 2019, The Authors, published by Springer Nature. b) A reversible, bidirectional shape-memory effect (rbSME) in response to programmed temperatures and demonstration of a transparent soft gripper via rbSME. Reproduced with permission.[70] Copyright 2013, Wiley-VCH. c) 3D-printing of ionic composite hydrogels and osmotically driven actuation. Reproduced with permission.[76] Copyright 2017, Wiley-VCH. d) Thermoresponsive actuation facilitated by permittivity switching in an electrostatically anisotropic hydrogel and the displacement profile of L-shaped hydrogel actuator upon heating/cooling. Reproduced with permission.[19] Copyright 2015, Springer Nature.

of its insolubility upon a low critical solution temperature behavior.[77,78] As a result, the dehydration occurs to induce large anisotropic electrostatic repulsive force between TiNSs nanosheets in PNIP. Thus, this actuator easily deforms along parallel and shear directions orthogonal to cofacial orientation of nanosheets while resisting compression (Figure 5d). Relying on this feature, an L-shaped actuator with PNIPA/TiNSs composite propels unidirectionally even with small change in its water content from open air condition (Figure 5d, bottom).

Unlike electrical driven actuators, these alternative types of actuators employ nonelectrical stimulus such as pressurized air/water, heat, and humidity for transparent materials to take movements. Though one has large power consumption compared to other actuation mechanisms, and another one comparably shows slow response time,[79,80] the developments of many available systems can allocate imperceptible actuating systems depending on specific situation or environments.

3. Transparent Soft Sensors

To sense external forces or to send out signals for controlling robots, soft sensors have been through many researches in both fields of electronic skin and soft robotics. Many colleagues in these field have come up with a variety of approaches to incorporate many kinds of perceptions in soft and stretchy features.[21,24,81–83] Mechanical properties of such perceptions similar to human skin are taken as a standard to develop soft electronic sensors. Therefore, the strategies to transform materials into low Young's modulus that matches with skin are highly desirable and proposed in many studies. Reducing the thickness of the sensor is an important component in improving the mechanical suitability for all surfaces and mitigating the inconvenience of human or robot integration. Moreover, in similar ways, our typical interest in optical transparency of the sensors can be realized in two ways: patterning or intrinsic property of materials. In this regard, we review recent advances in realizing transparent soft sensors with both mechanically and visually imperceptible in the following section and summarize their performance parameters as sensors in **Table 2** with respect to their design principles.

3.1. Patterning Enabled Transparent Soft Sensor

Although intrinsic stiffness of materials often constrains in strain elongation, electronics with extreme level of thinness interface well with curvilinear and dynamic surfaces, thereby thriving the advances in functionality of imperceptible electronic skins as well as robotic perceptions. Ultrathin film electronics usually with a thickness within a few single micrometers and down to 300 nm offer ultralightweight and unobstructive physical properties, establishing imperceptible tactile sensor arrays and PLEDs that can conform to the skin in wrinkled or crumpled manner without disturbing the performance (**Figure 6**a).[84–87] As a prime example, Someya's group has first reported ultrathin electronics with patterned active matrix pressure sensor arrays of organic field-effect transistors (OFETs) fabricated on a 1.3 µm thick, ultralight plastic substrate, demonstrating mechanical imperceptibility and pressure sensing capability that can be used in biomedical systems as well as a robotic skin.[84] Though ultrathin electronics exhibits mass per area.

By engineering thin films into elastically deformable patterns, it offers mechanical compliances and optical transparency

Table 2. Transparent soft sensors.

Design principles	Materials used	Functions	Electrical property	Sensitivity	Detection range	Response time	Transparency (%)	Stretchability (%)	Thickness	Ref.
Patterning enabled transparent soft sensor										
Ultrathin film	Au/parylene	Pressure	–	–	0–1 kPa	–	–	60	300 nm	[86]
	PEDOT:PSS/PEN	Temperature, pressure	130 $\Omega\ \square^{-1}$	–	0–1 kPa	–	–	275	14 µm	[87]
	OTFT/PEN	Pressure, strain, infrared	–	–	0–1 kPa	–	–	230	1.3 µm	[84]
Serpentine pattern	IZO/Au/PI	UV/temperature/strain	–	GF: 2.11	0–30%	26.6 µs	–	30	4 µm	[22]
	Graphene/PMMA	Strain, electrophysiology, hydration, temperature	1994.3 ± 264 $\Omega\ \square^{-1}$	GF: 5	0–50%	–	85	50	463 ± 30 nm	[81a]
	AgNWs/PDMS	Electrophysiology, heater	5.6×10^6 S m^{-1}	–	–		–	30	300 µm	[88]
	Au/PI	Pressure, strain, electrophysiology, temperature	–	10 kPa^{-1}	0–10 kPa	–	–	30	5 µm	[24]
Microfluidic elastomers	Channel: PDMS Fluid: Galinstan/Cu	Strain, proximity	2.95 Ω	GF: 0.01	0–150%	–	>85	>100	600 nm (300 µm w/substrate)	[96]
	Channel: Ecoflex Fluid: EGaIn	Strain	2.6–3.1 Ω	100 kPa^{-1} GF: 0.007	50–100 kPa 0–100%	–	–	≈900	3.5 mm	[93]
	Channel:PDMS Fluid: EGaIn	Pressure, strain	10 Ω	100 kPa^{-1}	100 kPa 0–300%	–	–	350	700 µm	[99]
Kirigami structure	AgNWs/cPI	Temperature, electrophysiology	<50 $\Omega\ \square^{-1}$	–	–	–	>85	≈400	5 µm	[102]
	Graphene/PI	Photodetector	–	–	–	–	–	≈240	4–20 µm	[103]
Intrinsically transparent soft sensor										
Ionic skin	PAAm hydrogel	Pressure, strain	1 S cm^{-1}	–	0–100%	20 ms	98	≈1000	4 mm	[82]
	PEGDA hydrogel	Pressure	1.27×10^{-7} S cm^{-1}	–	0–300%	–	92.4	≈1100	1 mm	[107]
	NaCl in EG/Ecoflex	Strain	2.72 × 10–1 S m^{-1}	GF: 4	0–250%	–	–	300	3.3 mm	[108]
Polymer engineering	PEDOT:PSS/ micropatterned PDMS	Strain	130 $\Omega\ \square^{-1}$	0.9 kPa^{-1}	5–20 kPa	140 ms	74	30	2.7–6.8 µm	[151]
	PEDOT:PDSS/PU	Strain	63 $\Omega\ \square^{-1}$	–	0–20%	–	–	20	150 nm (1 mm w/substrate)	[89]
	STEC-doped PEDOT:PSS	Pressure, strain	100– 4300 S cm^{-1}	–	0–300%	–	75–95	0 – 600	500 nm (200 µm w/ substrate)	[81b]
Percolation network	AgNWs/TPU	Strain	20.8 $\Omega\ \square^{-1}$	GF: 20–337	0–80%	–	80–91	80	10–41 µm	[116]
	Ag/PVA NF	Pressure	1.68–11.1 $\Omega\ \square^{-1}$	–	4.4 Pa	70 ms	≈70	≈100	–	[115]
	PUU/AgNWs/PDMS	Strain	11.01 $\Omega\ \square^{-1}$	–	0–230 kPa 0–35%	–	90.6	100	170 µm	[152]
	CNTs/PDMS	Pressure, strain	1100–2200 S cm^{-1}	–	0–200% 0–50 kPa	–	88–95	≈150	300 µm w/substrate	[112]

across a wide range of materials, including metals employed in industries (such as gold, copper, and silver) as well as nanomaterials (e.g., Ag nanowires, graphene, etc.) (Figure 6b).[22,24,81,88,89] Examples of these deterministic patterns range from filamentary serpentine circuits to self-similar fractal structures.[21,90] The common subtractive/additive ways to pattern thin films ensure both transparency and mechanical deformability through the formation of open-mesh structures in wavy form. In contrary to the other sensors, these pattered electrodes are usually made of noble metals that are nonirritating to skin, so the range of applications for this sensor has been from collecting health monitoring to tactile feedback system.[22,24] Many of these designs incorporate circuits on mechanically neutral plane layouts either by underlying of thermoplastic polymer or encapsulation of entire circuits. Using the thinnest conductive material in the world, graphene, one work has reported the graphene electronic tattoo (GET) designed as filamentary serpentines.[81a] The GET has the total thickness in hundreds of nanometers including the support layer, high optical transparency (≈85%), and stretchability (≈40% of strain). In particular, the GET has been further applied to measure electrooculography around a human eye, which is a

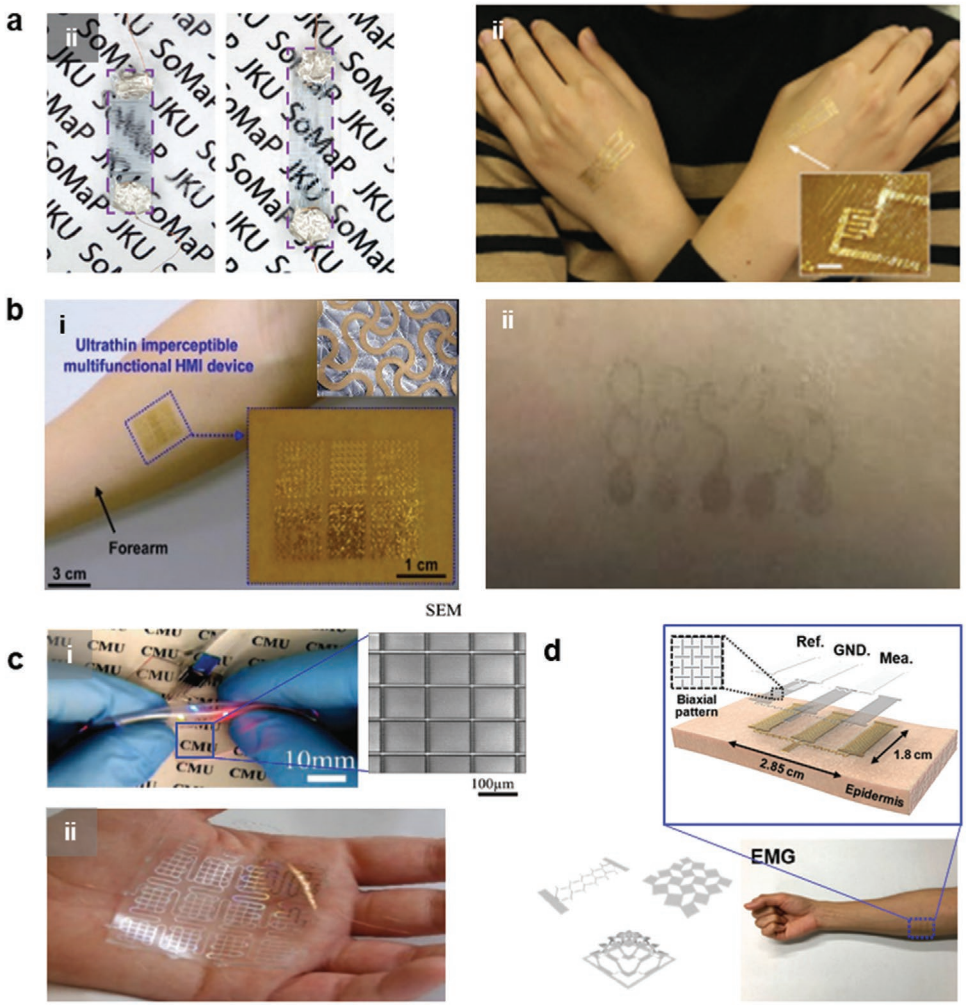

Figure 6. Patterning enabled transparent soft sensors. a) Ultrathin electronics: i) ultrathin and transparent conductor with prestrained structure; ii) sub-300 nm-thick imperceptive sensors. a-i) Reproduced with permission.[87] Copyright 2015, Wiley-VCH. a-ii) Reproduced with permission.[86] Copyright 2016, Wiley-VCH. b) Deterministic serpentine design: i) metal oxide semiconductor nanomembrane for unnoticeable multifunctional human–machine interfaces (HMIs); ii) graphene electronic tattoo (GET). b-i) Reproduced with permission.[22] Copyright 2019, The Authors, published by AAAS. Reprinted/adapted from ref. [22]. © The Authors, some rights reserved; exclusive licensee American Association for the Advancement of Science. Distributed under a Creative Commons Attribution NonCommercial License 4.0 (CC BY-NC) http://creativecommons.org/licenses/by-nc/4.0/. b-ii) Reproduced with permission.[81a] Copyright 2017, American Chemical Society. c) Microfluidic elastomers: i) visually imperceptible biphasic (solid–liquid interface) stretchable electrode; ii) soft tactile keypad. c-i) Reproduced with permission.[96] Copyright 2018, Wiley-VCH. c-ii) Reproduced with permission. c-ii) Reproduced with permission.[99] Copyright 2011, IEEE. d) Kirigami designs: kirigami engineering of silver nanowire (AgNW)/colorless polyimide (cPI) composite. Reproduced with permission.[102] Copyright 2019, American Chemical Society.

prominent area for appearance with delicate skin. Moreover, the potential advantage of the imperceptible GET is confirmed by applying the GET for human–robot interface to wireless control a quadcopter in real time without user's discomfort in a completely unobstructed manner.[91] In other work, thin metal oxide nanomembrane (under sub-micrometers) incorporating aforementioned metal circuits in deterministic design is used as highly sensitive sensors in human–machine interactions device.[22] Thus, mechanically and visually imperceptible property of thin, highly definable, and open-mesh structure in deterministic design greatly attributes to be utilized as transparent soft sensors in imperceptible robotic applications.

Taking microfluidic elastomer to fabricate the soft sensor has been a very reliable approach ever since the rise of soft robotics (Figure 6c). Most of microfluidic elastomers is fabricated by vacuum assisted injection of conductive liquid materials into predefined microchannel geometries, enabling the fabrication of soft sensors with a simple, reproducible, and reliable manner.[92,93] Liquid metals are conductors that are deformable like liquid at room temperature. Their unusual properties stem from eutectic binary phase of an alloy with different metals. EGaIn has been particularly desirable material for these applications because of its high conductivity, low viscosity, and low toxicity at vapor pressure.[94,95] Among the microfluidic elastomer utilizing liquid metals, a few fabrication approach called, "biphasic thin film conductor" has been developed. It is the method by which a thin layer of liquid metal on face-centered-cubic (FCC) metals (typically gold, copper, and silver)[96–98] forms an alloy, usually with gallium-based liquid metals, with the aid of an aqueous NaOH solution. This fabrication method not only take soft stretchy compliance of microfluidic elastomer but also significantly reduces the resolution the liquid metal traces down to sub-micrometer scale (<5 µm) in width, so the electrode in an array form may look visually imperceptible and transparent.[96] Although a biphasic thin film normally has a thickness in hundreds of nanometers including both a thin FCC metal and a liquid-metal layer together, it has to be encapsulated with a soft elastic layer to preserve the coated liquid-metal layer within the structure. These various types of compliant soft microfluidic elastomer devices can be used for pressure/strain sensing for tactile feedback in a form of keyboard or artificial soft skin.[93,99,100] Although they have a low gauge factor and sensitivity, their mechanically robustness and ultrastretchability makes them very compelling for the large deformable joints and highly durable tasks.[101] On the other hand, a trade-off for having superior mechanical stability can be critical as sensors. Microfluidic-elastomer-based soft sensors typically exhibit a thickness of over 100 µm to millimeters, depending on the thickness of the channel and the height of the liquid-metals trace, thereby limiting the mechanical compliance to other interfaces, compared to the aforementioned sensors. Even if these limitations can be overcome by continued research while maintaining the original superiority of the microfluidic-elastomer-based soft sensors, it has the greatest potential utilized over conventional soft conductive materials and forged into a strong candidate for stretchable sensors in constructing transparent perception systems for imperceptible soft robotics.

The ancient art of repetitive paper cutting, called kirigami, offers a simple way to engineer a flat sheet into elastically stretchable form (Figure 6d). Recent reports have engineered flexible transparent conductors made of silver nanowires/colorless polyimide (cPI) or graphene/poly(methyl methacrylate) (PMMA) into stretchable and transparent sensor electrodes by employing kirigami approach.[102,103] These kirigami engineered patterns impart tunable elasticity to the electrodes, which can be easily modulated depending on applications over the range of 0 to over 400% tensile strain with strain-invariant electrical property and excellent strain reversibility. In such works, the electrodes can patterned either by computer aided design system using laser ablation or by conventional photolithography. Although this approach is inappropriate for mechanical tactile sensing due to its strain invariant characteristic, it may be useful in rapid prototyping patterned conformal electrodes for electrophysiology measurements and for providing stable circuit for deformable objects in imperceptible soft robotics.

3.2. Intrinsically Transparent Soft Sensor

Many conductive materials, such as metals and carbons, are often constrained by stiffness, brittleness, and opacity when it comes to manufacture transparent soft sensors. However, great advances have been made in the development of materials that are intrinsically soft and stretchy for use as transparent soft sensors. In this section, intrinsically transparent soft sensors engineered in various ways will be discussed.

Ionic skins are ionically conductive transparent sensors made of loosely crosslinked polymeric chains that are filled with water or other ionic liquid (**Figure 7**a).[82] By filling desired solutions with different ions, electrical or mechanical properties of the material can be tuned to serve as transparent stretchable conductors/transistors that can also deform into arbitrary shapes.[104,105] Although the electrical conductivity for ionic conductor (10^{-2}–10^{3} S m^{-1}) usually is not as great compared to other materials that make up the other proposed sensors, such conductivity value has been enough to allow for Kim et al. to demonstrate highly compliant device that mimics sensory system very similar to what human skin is composed, called “ionic touch panel.”[82,106] The surface capacitive touch system is demonstrated to show robustness of the panel during the operation under mechanical strain up to 1000% areal strain. Although the tough gels are mechanically compliant and biocompatible, they can eventually malfunction when exposed to air on the long-term. Recently, one work has demonstrated ionically conductive elastomer (ICE) that is capable resisting to high temperature as high as 200 °C and making a circuit comparable to metals.[107] Also another work has taken a concept of a microfluidic elastomer to incorporate an ionic liquid (ethylene glycol (EG)/NaCl) injected into the microchannel.[108] This work enabled hysteresis-free strain sensing by taking advantage of the fully encapsulated structure ionic liquid (ethylene glycol) with high evaporation temperature (<190 °C) without leakage. As a result, ionic conductors are still strong candidates for transparent sensory system as long as continuous research on the evaporation issue of their fillers can be solved.

Polymer engineering can also be solutions to grant to mechanical compliance similar to tactile system of human/robotic skin. Polymer engineering involves doping of specific conductive polymers to give conductive pathways by bindings for electrical conductivity and enriching the ionic transportation by filling in cations with better ionic conductivity.[109] Among many of conductive polymers, PEDOT:PSS with additives has been extensively employed as the most common conductive polymer due to its high electrical conductivity and hole transport mobility for organic solar-cells, touch panels, and mechanical sensors.[89,110,111] Several groups have formulated such additives the combination of dimethyl-sulfoxide and Zonyl fluorosurfactant or stretchability and electrical conductivity (STEC) method to ensure ubiquity of PEDOT:PSS in applications demanding mechanical flexibility and transparency.[89] With forementioned strategies, circuits that are semi-transparent and electrically conductive close to metals can also be developed (Figure 7b).[50] The ongoing challenge in polymer engineering in developing transparent soft sensors seems to be conductivity, transparency, and mechanical deformability. Although alternative design principles or materials have other constraints, transparent soft sensors made out of previous approaches have not fully exceeded the highest performance in comparison to other approach from above-mentioned criteria. Conductive polymers blended with different doping elements may seek to overcome the performance as well as durability for implementation in imperceptible soft robotics parts.

In the field of nanotechnology, material with 1D structure refers to a wire-shaped material with a nanometer thickness that bends and deforms in universal directions with excellent

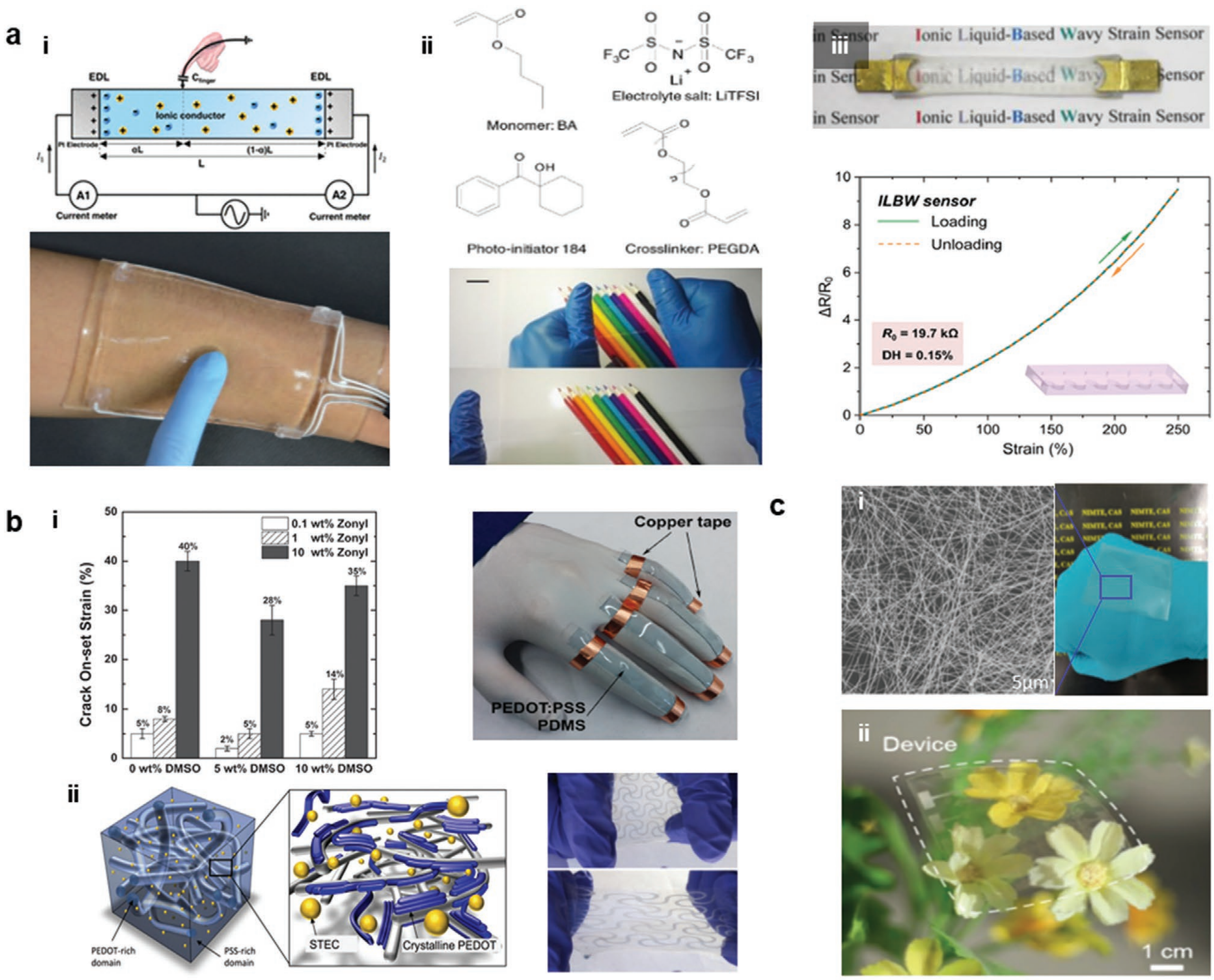

Figure 7. Intrinsically transparent soft sensors. a) Ionic conductive elastomers: i) Ionic touch panel application with a surface capacitive system. ii) Ionic conductive elastomer (ICE) with enhanced thermal stability and electrical conductivity. iii) Ionic-liquid-based wavy (ILBW) strain sensor with hysteresis-free strain sensing capability. a-i) Reproduced with permission.[82] Copyright 2016, AAAS. a-ii) Reproduced under the terms of the CC-BY Creative Commons Attribution 4.0 International License (https://creativecommons.org/licenses/by/4.0).[107] Copyright 2018, The Authors, published by Springer Nature. a-iii) Reproduced with permission.[108] Copyright 2017, American Chemical Society. b) Conductive polymers: i) Effect of Zonyl as an additive to PEDOT:PSS for improved transparent mechanical sensors. ii) Stretchability and electrical conductivity (STEC) enhancer assisted transparent and stretchable circuits and sensors. b-i) Reproduced with permission.[89] Copyright 2015, Wiley-VCH. b-ii) Reproduced with permission.[81b] Copyright 2017,The Authors, published by American Association for the Advancement of Science (AAAS). Reprinted/adapted from ref. [81b]. © The Authors, some rights reserved; exclusive licensee American Association for the Advancement of Science. Distributed under a Creative Commons Attribution Non-Commercial License 4.0 (CC BY-NC) http://creativecommons.org/licenses/by-nc/4.0/. c) Percolation network: i) AgNWs/PU-based mechanical sensor for human motion monitoring. ii) Highly stretchable and transparent triboelectric tactile sensor with percolated electrospun Ag-nanofiber electrodes. c-i) Reproduced with permission.[116] Copyright 2019, The Royal Society of Chemistry. c-ii) Reproduced with permission.[115] Copyright 2018, Wiley-VCH.

mechanical flexibility. These 1D-nanomaterials, consisting of carbon,[112] metals,[113] and semiconductors,[83] can be advantageous with various aspects. Percolation network typically refers to a network that is randomly distributed in a specific area. This structure enables to deform with a mechanical strain while maintaining transparency and electrical conductivity by connected wire–wire junctions in opened and web-like geometry. Transparent conductors in percolation system can induce the change in resistance arises from the contact resistance at each crosslinked joints, which vary with deformations (Figure 7c). These sensors are often well-suited for wearable devices and can be used to determine spatial position and joint angles as well.[81b,114–116] Mesh structures in nanoscales formed by the deposited gold, copper, or silver on polymeric fibers such as poly(vinyl alcohol) and polyurethane can be integrated directly onto the skin or any surfaces in a form of tattoo, ensuring conformability and gas-permeability while functioning as sensors for measuring motions and electrical signals.[117–120] Besides, by taking the advantages of many available 1D-nanomaterials materials that fits in electrical work function alignment, Kim et al. have constructed an all-nanowires transistor for intrinsically stretchable mechanical perception system in a soft robotic hand.[83] Tactile sensory system using 1D material based percolation network has high sensitivity and a gauge factor in response to mechanical stimuli. The sensors with nano/micro-range materials suffer chemical/mechanical durability issues in long-term/cyclic operations. Current research on such issues includes finding protective matrix materials, plating/coating with nanomaterials with higher stability and so on.[121,122]

4. Imperceptions through Camouflage

Programmable camouflage system can be a successful alternative to the transparent materials. These structures can be imperceptible through mimicking their surrounding environments by altering their skin color and morphology. The earliest camouflage soft robot was created by the scientists at Harvard and Defense Advanced Research Projects Agency (DARPA), which is capable of tuning its skin color into their backgrounds and even hiding in the infrared region.[13] The coloring elements inside the pneumatic soft robot have been provided by open-ended microchannels. As shown in **Figure 8**a, the robot is actively camouflaged as the robot moves toward the rock. The soft robot is also capable of IR camouflage by injecting highly thermal conductive materials into the channel.

Inspired by the camouflageable systems in Cephalopod, recent study developed a stretchable multimodal camouflage platform with multispectral region.[123] In order to do so, researchers used a trilayer system of acrylate elastomer substrate covered with wrinkled pentablock copolymer. As shown in Figure 8b, the irregular wrinkled surface of the pentablock copolymer is flattened by the equiaxial strain applied by the DEA actuating system and making the entire system to be transparent in visible to IR range. These active camouflage platforms may enable adaptive transformation, which change its skin from transparent to specific colors.

A fast color shift (refresh speed under 1 s) can be achieved by the nanosized geometric feature deposited with gold (Au).[124] Electrodeposition system consisting of gel electrolyte, Pt electrode, and nanodome arrays enables active color shifting structure. An intrinsic plasmonic spectral properties of the dome-like structure leads to blueshift, and the deposition thickness of the Au leads to redshift of the structure. These plasmonic

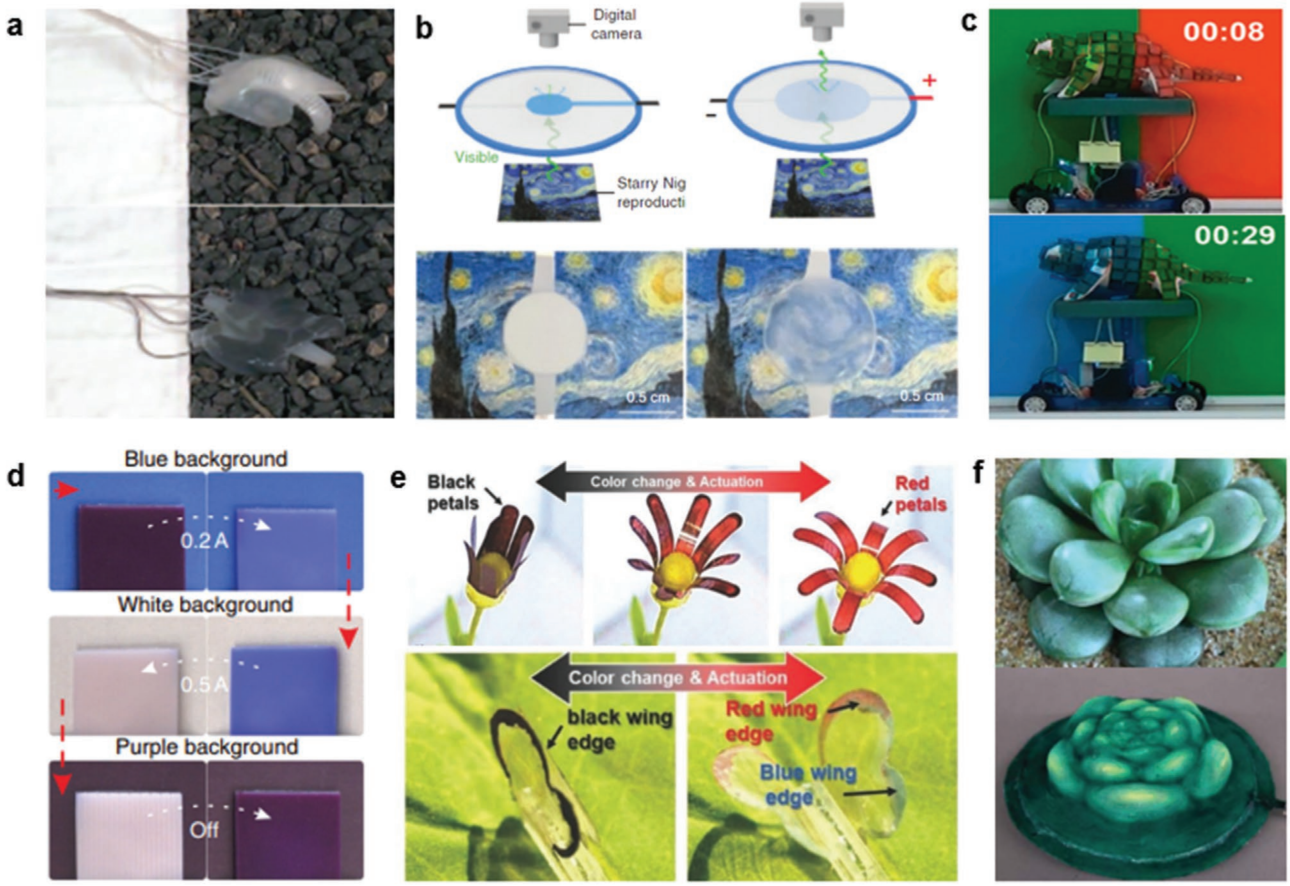

Figure 8. Advances in materials for camouflageable skins. a) Soft machines camouflaged by injection of pigments. Reproduced with permission.[13] Copyright 2012, AAAS. b) Stretchable multimodal camouflage platform inspired by cephalopods. The wrinkled copolymer structure enables tunable transparency. Reproduced with permission.[123] Copyright 2020, Wiley-VCH. c) Active color shifting skin by the plasmonic spectral properties of electrodeposited gold and nanoarrays. Reproduced with permission.[124] Copyright 2016, American Chemical Society. d) Stretchable color-shifting skin with a thermochromic elastomeric skin and an embedded liquid-metal heater. Reproduced under the terms of the CC-BY Creative Commons Attribution 4.0 International license (https://creativecommons.org/licenses/by/4.0).[146] Copyright 2019, The Authors, published by Springer Nature. e) Simultaneous anisotropic and color-shifting actuation of a biomimetic actuator. Reproduced with permission.[130] Copyright 2018, Wiley-VCH. f) Programmable robotic tissue mimicking the surrounding environments. Reproduced with permission.[25] Copyright 2017, AAAS.

Table 3. Environmentally adaptive camouflageable skins.

Adaption ability	Materials used	Structure	Working principle	Activation power	Ref.
Active infrared and visible radiation	Dye and pigment	Soft robot with microfluidic channel	Pigment microfluidic injection	2.25 mL min^{-1}	[13]
Active visual and infrared camouflage	Pentablock copolymer	Wrinkled structure of copolymer	Mechanical Strain applied by DEA	3.5 kV	[123]
Active visual camouflage	Gold and silver	Nanodot array	Plasmonic modulation	1.5 V electrodeposition	[124]
Active visual wavelength color shifting	Silica particles	Silica particles embedded in elastomer	Mechanochromic	0–60% strain	[128]
Active color change with actuation	Thermochromic microcapsule dye	Dye coated over transparent metal nanowire layer	Thermochromic	0–15 V	[130]
Full color camouflage	Cholesteric liquid-crystalline polymer	Inkjet printed photonic polymer	Controlling nonreactive mesogen	Controlling ion concentration	[127]
Brown to yellow green	Fe_3O_4@C	Photonic crystal/EG in PDMS fiber channel	Photonic crystal magnetic field actuation	Magnetic field	[125]
Controllable color shifting	Amorphous silicon (a-Si)	a-Si deposited on reflective metal substrate	Eletro-chemomechanical control	0–1.5 V	[153]
Color visualization and camouflage response to environment cues	Theromochromic, halochromic, phosphorescent dyes	Sensitive dyes coated on soft body	Temperature, pH, and light sensitive dye	Temperature, pH, and light	[154]
Flexible optoelectronic camouflage (black to white)	Thermochromic dyes	Thermochromic dye with Joule heating ultrathin silicon	Thermochromic	15 V	[155]
Active color shifting by external strain (0–140%) and pressure	Thermochromic dye	Thermochromic dyes heated by a liquid-metal microfluidic channel	Thermochromic	0.5 A	[146]
Programmable 3D shape morphing to surrounding environment	Silicone elastomer	Silicone elastomer patterned with fabric pattern	3D shape morphing	Pneumatic	[25]

cells covering the chameleon robot actively control the skin color by altering the deposition voltage. As shown in Figure 8c, the artificial chameleon recognizes the background color and automatically changes its color in a few second. Various active color changing materials are further developed using magnetic,[125] temperature,[126] water,[127] and mechanical strain[128] (**Table 3**). Recently, a color shifting material in a stretchable form has been developed using liquid metal and thermochromic pigment (Figure 8d).[129,146] Embedded liquid metal inside the elastomer provides Joule heating to the thermochromic liquid crystal layer. The device can be used as a visual indicator of an external stimuli since the electrical resistance varies by the strain or pressure.

An advanced form of integrated system of color shifting skin with soft actuator has been demonstrated by integrating thin film soft actuator and thermochromic dye (Figure 8e).[130] Percolative networks of metal nanowires provide heat to the bilayer polymers of LDPE and poly(vinyl chloride) (PVC). Anisotropic motion in actuation is occurred through the different thermal expansion coefficient of the two materials. Joule heating provided during the actuation simultaneously changes the color of the thermochromic layer deposited above the actuator.

Recent research introduced a programmable robotic tissue, which transforms 2D surfaces into targeted 3D shapes inspired by the morphology change from the cephalopod.[25] By combining two materials, fiber mesh and stretchable elastomer, the mesh provides force toward the axis of the actuator and controls the shape, whereas the elastomer is connected between the fiber meshes acting as a stretchable tissue. By controlling the distance between the fiber meshes, they successfully mapped a 3D shape into 2D surface. When this soft robotic tissue is inflated at a given pressure, the pattern pops up into the structure imitating various shapes such as the high-aspect-ratio plant containing nonsymmetric leaves (Figure 8f).

As majority of the camouflage abilities are driven by thermal and external strain (stretch, pneumatic, electric), development of decoupling the effect of external stimuli is crucial. Moreover, sophisticated integration with the soft body considering the external wirings, channels, and power source remains challenging.

5. Current Challenges and Perspectives

Various strategies from recent progress of transparent sensors, actuators, and also camouflageable skins enable the development of an integrated imperceptible system which may offer great potentials in various applications such as undercover operations[130,131] and wearable assistive devices.[132,133] Despite all the recent improvements, there are several considerable works to be done for practical use. We can envision integration of sensors and actuators, self-powered automacy through various chemical and biological energy sources, and new levels of sensor signal identification by integration with machine intelligence. Our perspectives on imperceptible soft robotics for further developments would include the following contents (**Figure 9**).

5.1. Integrated System of Sensors and Actuators

An ultimate stage of an imperceptible soft body will be combined by three main parts; a soft actuator, soft sensory systems, and soft functional skin. Soft sensors are integrated with the robots in order to sense external stimuli. Also, the sensors for soft robot

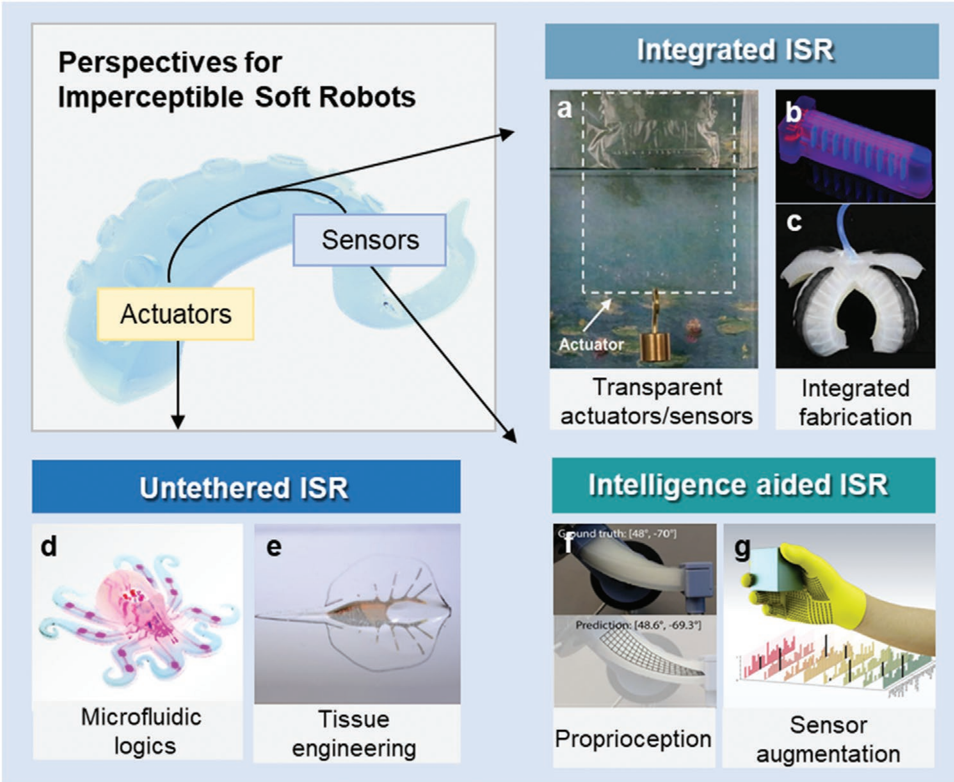

Figure 9. Perspective of imperceptible soft robotics (ISR) from addressing the current goals to resolving current problems. a) A transparent actuator/sensor combined system. Reproduced with permission.[134] Copyright 2018, The Authors, published by AAAS. b) Proprioceptive and tactile measurement of inflation, curvature, and contact by embedded ionic gel with 3D printing of sensors and actuators with seamless junction. Reproduced with permission.[135] Copyright 2018, Wiley-VCH. c) Integrated fabrication of sensors and actuators through ethanol-based solvent. Reproduced with permission.[136] Copyright 2020, The Authors, published by AAAS. d) Autonomous operation through chemical decomposition. Reproduced with permission.[137] Copyright 2016, Springer Nature. e) Tissue-engineered cardiomyocytes with untethered actuation. Reproduced with permission.[138] Copyright 2016, AAAS. f) Soft robotic proprioception aided by machine intelligence. Reproduced with permission.[142] Copyright 2018, The Authors, published by AAAS. g) Large-area multiobject detection through a machine-learning glove. Reproduced with permission.[143] Copyright 2019, Springer Nature.

proprioception are used to fully understand and track the shape of the soft body and therefore enables to better control.

Integrated transparent soft robotic system was firstly shown by Keplinger's group as shown in Figure 9a.[134] As explained in Figure 4a, the actuation is driven by the electrostatic forces and the real-time state of the system can be easily provided by the capacitance measurement of the electrodes.

Another work has 3D printed somatosensitive actuators for soft robotic proprioception, where the embedded ionic gel is printed along the actuator and enables proprioceptive feedback (Figure 9b).[135] Important feature of this device is that they assign separate sensors to three distinctive motions: inflation, curvature, and contact. The sensors for inflation and curvature efficiently measure the current state of the soft robot, and the contact sensor independently identifies the external object while grasping. Moreover, by compensating the conductance change occurred by the temperature difference, the system reliably detects identical objects with different temperatures. Moreover, the device is manufactured through unified fabrication which enables seamless junctions between different components. Developing the combined fabrication method and materials will be important on advancements on developing integrated transparent system.

Sensors and actuators of the integrated system require sophisticated analysis of structural design and material selection to attain optical transparency. Visually and mechanically imperceptible sensors and actuators can be easily integrated through physical attachment of each component. However, in some cases, compatibility of each fabrication methods of sensors and actuators could be critical issue on device integration. Combined fabrication may cause swelling or decomposition of neighboring materials on account of incompatible temperature and chemical ingredients. Ethanol-based conductive composite rather than conventional solvents such as toluene or cyclohexane could prevent decomposition of the prefabricated actuator (Figure 9c).[136] This introduces new approach not by simply combining each components but by integrating in the fabrication step.

5.2. Autonomous Operation with Imperceptibility

Development of an integrated power source with stretchable circuit system is crucial on independent soft robot operation. There is considerable recent process on transparent and flexible power source which could be integrated with the soft body. Using the decomposition energy of a chemical compound inside the flexible channel is a considerable candidate since it could achieve both the transparency and self-powered autonomous operation ability (Figure 9d).[137] Combining tissue-engineered cardiomyocytes (Figure 9e)[138] and actuator-battery combined energy-storage system[139] would also facilitate the autonomy of the soft robotic system.

5.3. Intelligence Aided Sensory Systems

Moreover, besides that the developed soft sensors are critical to hysteresis, they are also sensitive to unwanted external stimuli. Therefore, decoupling these signals remains challenging to guarantee stable operations. A single line of sensory circuit with deep learning data processing could identify the touch areas by creating different circuit patterns on each point.[140] These designs would allow discrimination of signals generated from multiple areas. Unfortunately, most of the soft sensors suffer from nonlinear outputs and hysteresis which make them difficult to integrate with the actuating system. Moreover, since a single sensor could not define the state the multidimensional system of soft actuator, the state monitoring of the soft structure is very challenging.

As an example of recent progress, a machine-learning approach is used to model the nonlinearities of the sensors in various dynamic motions. For example, Meerbeek et al. used long short-term memory networks in order to identify time series data and successfully demonstrated a model-free multimodal sensing by predicting the position and the applied force to the actuator.[141] Moreover, another research embedded 30 optical fibers inside a soft actuator, identifying a more complicated motions such as bending and twisting (Figure 9f).[142]

Moreover, sensory networks are necessary for large-area sensing and detection of various objects. Beyond the scope of conventional methods for measuring object, sensor combined with machine intelligence could provide both the grasping force and the identity of an object (Figure 9g).[143] The collected pressure map from a sensory array provides an image data that can enter the convolution network and enables to extract the identity of the object from the latent space.

6. Conclusion

Recent advancements in the development of new materials and designs in soft actuators and soft sensors now aim to push forward an ultimate goal that yields new technological demands by merging two similar research fields (soft robotics and wearable devices) together. Herein, we have introduced a new class of soft robotics, imperceptible soft robots (ISR), by addressing current state of arts in their three main hardware components: transparent soft actuators and sensors as well as camouflage skins—and describing the importance of imperceptibility in a new class of applications, such as undercover operative soft robots, assistive device, soft robotic prosthetics, and human–machine-interactive wearable devices. Simultaneous understanding of advantages and current challenges in current soft robotic system efficiently have led to complementary implementation of existing technologies of electronic skin and to develop further toward a paradigm shift to the new class of applications in the field of soft robotics. Such advancements will involve continued advances in transparent soft functional materials and new strategies in sensing, actuation, and camouflage skin integration for advanced optical and mechanical imperceptive properties.

Acknowledgements

P.W., K.K.K., and H.K. contributed equally to this work. This work was supported by a National Research Foundation of Korea (NRF) Grant funded through the Basic Science Research Program (2017R1A2B3005706).

Conflict of Interest

The authors declare no conflict of interest.

Keywords

camouflage skins, imperceptible robotics, soft robotics, transparent soft actuators, transparent soft sensors

Received: April 7, 2020
Revised: May 31, 2020
Published online:

[1] R. F. Shepherd, F. Ilievski, W. Choi, S. A. Morin, A. A. S tokes, A. D. Mazzeo, X. Chen, M. Wang, G. M. Whitesides, *Proc. Natl. Acad. Sci. USA* **2011**, *108*, 20400.
[2] M. T. Tolley, R. F. Shepherd, B. Mosadegh, K. C. Galloway, M. Wehner, M. Karpelson, R. J. Wood, G. M. Whitesides, *Soft Rob.* **2014**, *1*, 213.
[3] C. Larson, B. Peele, S. Li, S. Robinson, M. Totaro, L. Beccai, B. Mazzolai, R. Shepherd, *Science* **2016**, *351*, 1071.
[4] N. N. G. Caleb Christianson, D. D. Deheyn, S. Cai, M. T. Tolley, *Sci. Rob.* **2018**, *3*, eaat1893.
[5] C. Lee, M. Kim, Y. J. Kim, N. Hong, S. Ryu, H. J. Kim, S. Kim, *Int. J. Control, Autom. Syst.* **2017**, *15*, 3.
[6] K.-J. Cho, J.-S. Koh, S. Kim, W.-S. Chu, Y. Hong, S.-H. Ahn, *Int. J. Precis. Eng. Manuf.* **2009**, *10*, 171.
[7] B. B. Kang, H. Lee, H. In, U. Jeong, J. Chung, K.-J. Cho, in *2016 IEEE Int. Conf. Rob. Autom. (ICRA)*, Piscataway, NJ, USA **2016**, https://doi.org/10.1109/ICRA.2016.7487562.
[8] J. Kim, M. Lee, H. J. Shim, R. Ghaffari, H. R. Cho, D. Son, Y. H. Jung, M. Soh, C. Choi, S. Jung, *Nat. Commun.* **2014**, *5*, 5747.
[9] M. T. Tolley, R. F. Shepherd, B. Mosadegh, K. C. Galloway, M. Wehner, M. Karpelson, R. J. Wood, G. M. Whitesides, *Soft Rob.* **2014**, *1*, 213.
[10] S. I. Rich, R. J. Wood, C. Majidi, *Nat. Electron.* **2018**, *1*, 102.
[11] J. Wang, M.-F. Lin, S. Park, P. S. Lee, *Mater. Today* **2018**, *21*, 508.
[12] J. Sone, Y. Matsumoto, Y. Yasuda, S. Hasegawa, K. Yamada, *J. Rob. Mechatronics* **2020**, *32*, 315.
[13] S. A. Morin, R. F. Shepherd, S. W. Kwok, A. A. Stokes, A. Nemiroski, G. M. Whitesides, *Science* **2012**, *337*, 828.
[14] C. Laschi, M. Cianchetti, B. Mazzolai, L. Margheri, M. Follador, P. Dario, *Adv. Rob.* **2012**, *26*, 709.
[15] P. Li, Y. Wang, U. Gupta, J. Liu, L. Zhang, D. Du, C. C. Foo, J. Ouyang, J. Zhu, *Adv. Funct. Mater.* **2019**, *29*, 1901908.
[16] B. Chen, J. J. Lu, C. H. Yang, J. H. Yang, J. Zhou, Y. M. Chen, Z. Suo, *ACS Appl. Mater. Interfaces* **2014**, *6*, 7840.
[17] H. Lee, H. Kim, I. Ha, J. Jung, P. Won, H. Cho, J. Yeo, S. Hong, S. Han, J. Kwon, S. H. Ko, *Soft Rob.* **2019**, *6*, 760.

[18] J.-Y. S. Christoph Keplinger, C. C. Foo, P. Rothemund, G. M. Whitesides, Z. Suo, *Science* **2013**, *341*, 984.
[19] Y. S. Kim, M. Liu, Y. Ishida, Y. Ebina, M. Osada, T. Sasaki, T. Hikima, M. Takata, T. Aida, *Nat. Mater.* **2015**, *14*, 1002.
[20] P. Maiolino, F. Galantini, F. Mastrogiovanni, G. Gallone, G. Cannata, F. Carpi, *Sens. Actuators, A* **2015**, *226*, 37.
[21] D.-H. Kim, N. Lu, R. Ma, Y.-S. Kim, R.-H. Kim, S. Wang, J. Wu, S. M. Won, H. Tao, A. Islam, *Science* **2011**, *333*, 838.
[22] K. Sim, Z. Rao, Z. Zou, F. Ershad, J. Lei, A. Thukral, J. Chen, Q.-A. Huang, J. Xiao, C. Yu, *Sci. Adv.* **2019**, *5*, eaav9653.
[23] R. Dahiya, *Proc. IEEE* **2019**, *107*, 247.
[24] W. H. Yeo, Y. S. Kim, J. Lee, A. Ameen, L. Shi, M. Li, S. Wang, R. Ma, S. H. Jin, Z. Kang, *Adv. Mater.* **2013**, *25*, 2773.
[25] J. Pikul, S. Li, H. Bai, R. Hanlon, I. Cohen, R. Shepherd, *Science* **2017**, *358*, 210.
[26] J. D. Carrico, T. Tyler, K. K. Leang, *Int. J. Smart Nano Mater.* **2017**, *8*, 144.
[27] Y. Yang, Y. Wu, C. Li, X. Yang, W. Chen, *Adv. Intell. Syst.* **2019**, *2*, 1900077.
[28] G. M. Whitesides, *Angew. Chem., Int. Ed.* **2018**, *57*, 4258.
[29] A. Miriyev, K. Stack, H. Lipson, *Nat. Commun.* **2017**, *8*, 596.
[30] C. Majidi, *Adv. Mater. Technol.* **2018**, *4*, 1800477.
[31] M. Shahinpoor, H.-J. Schneider, *Intelligent Materials*, Royal Society of Chemistry, Cambridge, UK **2007**.
[32] O. Erol, A. Pantula, W. Liu, D. H. Gracias, *Adv. Mater. Technol.* **2019**, *4*, 1900043.
[33] S. Agarwal, S. Jiang, Y. Chen, *Macromol. Mater. Eng.* **2018**, *304*, 1800548.
[34] J. Kim, J. W. Kim, H. C. Kim, L. Zhai, H.-U. Ko, R. M. Muthoka, *Int. J. Precis. Eng. Manuf.* **2019**, *20*, 2221.
[35] V. A. Ganesh, A. Baji, S. Ramakrishna, *RSC Adv.* **2014**, *4*, 53352.
[36] J. Mohd Jani, M. Leary, A. Subic, M. A. Gibson, *Mater. Des.* **2014**, *56*, 1078.
[37] C. Ohm, M. Brehmer, R. Zentel, *Adv. Mater.* **2010**, *22*, 3366.
[38] T. J. White, D. J. Broer, *Nat. Mater.* **2015**, *14*, 1087.
[39] Q. He, Z. Wang, Y. Wang, A. Minori, M. T. Tolley, S. Cai, *Sci. Adv.* **2019**, *5*, eaax5746.
[40] Y. Huang, J. Liang, Y. Chen, *J. Mater. Chem.* **2012**, *22*.
[41] I. K. Han, T. Chung, J. Han, Y. S. Kim, *Nano Convergence* **2019**, *6*, 18.
[42] L. H. Jiajie Liang, N. Li, Y. Huang, Y. Wu, S. Fang, J. Oh, M. Kozlov, Y. Ma, F. Li, R. Baughman, Y. Chen†, *ACS Nano* **2012**, *6*, 4508.
[43] S. Yao, J. Cui, Z. Cui, Y. Zhu, *Nanoscale* **2017**, *9*, 3797.
[44] W. Zhang, M. Weng, P. Zhou, L. Chen, Z. Huang, L. Zhang, C. Liu, S. Fan, *Carbon* **2017**, *116*, 625.
[45] I. A. Anderson, T. A. Gisby, T. G. McKay, B. M. O'Brien, E. P. Calius, *J. Appl. Phys.* **2012**, *112*, 041101.
[46] R. K. Ron Pelrine, Q. Pei, J. Joseph, *Science* **2000**, *287*, 836.
[47] K. Jun, D. Kim, S. Ryu, I. K. Oh, *Sci. Rep.* **2017**, *7*, 6091.
[48] M. Wissler, E. Mazza, *Sens. Actuators, A* **2007**, *138*, 384.
[49] R. K. Ron Pelrine, J. Joseph, R. Heydt, Q. Pei, S. Chiba, *Mater. Sci. Eng., C* **2000**, *11*, 89.
[50] B. Chen, Y. Bai, F. Xiang, J.-Y. Sun, Y. Mei Chen, H. Wang, J. Zhou, Z. Suo, *J. Polym. Sci., Part B: Polym. Phys.* **2014**, *52*, 1055.
[51] V. G. V. Nicholas Kellaris, G. M. Smith, S. K. Mitchell, C. Keplinger, *Sci. Rob.* **2018**, *3*, eaar3276.
[52] T. Hwang, Z. Frank, J. Neubauer, K. J. Kim, *Sci. Rep.* **2019**, *9*, 9658.
[53] T. Hwang, H.-Y. Kwon, J.-S. Oh, J.-P. Hong, S.-C. Hong, Y. Lee, H. Ryeol Choi, K. Jin Kim, M. Hossain Bhuiya, J.-D. Nam, *Appl. Phys. Lett.* **2013**, *103*, 023106.
[54] U. Kim, J. Kang, C. Lee, H. Y. Kwon, S. Hwang, H. Moon, J. C. Koo, J. D. Nam, B. H. Hong, J. B. Choi, H. R. Choi, *Nanotechnology* **2013**, *24*, 145501.
[55] H. Shigemune, S. Sugano, J. Nishitani, M. Yamauchi, N. Hosoya, S. Hashimoto, S. Maeda, *Actuators* **2018**, *7*, 51.
[56] A. Minaminosono, H. Shigemune, Y. Okuno, T. Katsumata, N. Hosoya, S. Maeda, *Front. Rob. AI* **2019**, *6*, https://doi.org/10.3389/frobt.2019.00001.
[57] E. Cakmak, X. Fang, O. Yildiz, P. D. Bradford, T. K. Ghosh, *Carbon* **2015**, *89*, 113.
[58] Y. R. Lee, H. Kwon, D. H. Lee, B. Y. Lee, *Soft Matter* **2017**, *13*, 6390.
[59] K. Jun, J. Kim, I. K. Oh, *Small* **2018**, *14*, 1801603.
[60] D. R. C. Mihai Duduta, R. J. Wood, in *IEEE Int. Conf. Rob. Autom.*, IEEE, Sigapore **2017**.
[61] Y. Chen, L. Agostini, G. Moretti, M. Fontana, R. Vertechy, *Smart Mater. Struct.* **2019**, *28*, 114001.
[62] S. K. Mitchell, X. Wang, E. Acome, T. Martin, K. Ly, N. Kellaris, V. G. Venkata, C. Keplinger, *Adv. Sci.* **2019**, *6*, 1900178.
[63] D. Stuart-Fox, A. Moussalli, *Philos. Trans. R. Soc., B* **2009**, *364*, 463.
[64] T. Li, G. Li, Y. Liang, T. Cheng, J. Dai, X. Yang, B. Liu, Z. Zeng, Z. Huang, Y. Luo, T. Xie, W. Yang, *Sci. Adv.* **2017**, *3*, e1602045.
[65] H. Yuk, S. Lin, C. Ma, M. Takaffoli, N. X. Fang, X. Zhao, *Nat. Commun.* **2017**, *8*, 14230.
[66] E. W. Hawkes, L. H. Blumenschein, J. D. Greer, A. M. Okamura, *Sci. Rob.* **2017**, *2*, eaan3028.
[67] K. Kobayashi, C. Yoon, S. H. Oh, J. V. Pagaduan, D. H. Gracias, *ACS Appl. Mater. Interfaces* **2019**, *11*, 151.
[68] C. Wu, J. Feng, L. Peng, Y. Ni, H. Liang, L. He, Y. Xie, *J. Mater. Chem.* **2011**, *21*, 18584.
[69] R. L. Andreas Lendlein, *Science* **2002**, *296*, 1674.
[70] M. Behl, K. Kratz, J. Zotzmann, U. Nochel, A. Lendlein, *Adv. Mater.* **2013**, *25*, 4466.
[71] R. Yang, Y. Zhao, *ACS Macro Lett.* **2018**, *7*, 353.
[72] L. Hines, K. Petersen, G. Z. Lum, M. Sitti, *Adv. Mater.* **2017**, *29*, 1603483.
[73] P. Zhou, L. Chen, L. Yao, M. Weng, W. Zhang, *Nanoscale* **2018**, *10*, 8422.
[74] J. Shang, P. Theato, *Soft Matter* **2018**, *14*, 8401.
[75] M. Behl, M. Y. Razzaq, A. Lendlein, *Adv. Mater.* **2010**, *22*, 3388.
[76] J. Odent, T. J. Wallin, W. Pan, K. Kruemplestaedter, R. F. Shepherd, E. P. Giannelis, *Adv. Funct. Mater.* **2017**, *27*, 1701807.
[77] H. G. Schild, *Prog. Polym. Sci.* **1992**, *17*, 163.
[78] F. Gómez-Galván, T. Lara-Ceniceros, H. Mercado-Uribe, *Meas. Sci. Technol.* **2012**, *23*, 025602.
[79] R. K. Katzschmann, A. de Maille, D. L. Dorhout, D. Rus, in *2016 IEEE/RSJ Int. Conf. Intelligent Robots and Systems (IROS)*, IEEE, Piscataway, NJ, USA **2016**, pp. 3048–3055.
[80] F. Hu, L. Lyu, Y. He, *Int. J. Precis. Eng. Manuf.* **2019**, *20*, 1915.
[81] a) S. Kabiri Ameri, R. Ho, H. Jang, L. Tao, Y. Wang, L. Wang, D. M. Schnyer, D. Akinwande, N. Lu, *ACS Nano* **2017**, *11*, 7634; b) Y. Wang, C. Zhu, R. Pfattner, H. Yan, L. Jin, S. Chen, F. Molina-Lopez, F. Lissel, J. Liu, N. I. Rabiah, Z. Chen, J. W. Chung, C. Linder, M. F. Toney, B. Murmann, Z. Bao, *Sci. Adv.* **2017**, *3*, e1602076.
[82] C.-C. Kim, H.-H. Lee, K. H. Oh, J.-Y. Sun, *Science* **2016**, *353*, 682.
[83] H.-J. Kim, K. Sim, A. Thukral, C. Yu, *Sci. Adv.* **2017**, *3*, e1701114.
[84] M. Kaltenbrunner, T. Sekitani, J. Reeder, T. Yokota, K. Kuribara, T. Tokuhara, M. Drack, R. Schwödiauer, I. Graz, S. Bauer-Gogonea, S. Bauer, T. Someya, *Nature* **2013**, *499*, 458.
[85] T. Yokota, P. Zalar, M. Kaltenbrunner, H. Jinno, N. Matsuhisa, H. Kitanosako, Y. Tachibana, W. Yukita, M. Koizumi, T. Someya, *Sci. Adv.* **2016**, *2*, e1501856.
[86] R. A. Nawrocki, N. Matsuhisa, T. Yokota, T. Someya, *Adv. Electron. Mater.* **2016**, *2*, 1500452.
[87] M. Drack, I. Graz, T. Sekitani, T. Someya, M. Kaltenbrunner, S. Bauer, *Adv. Mater.* **2015**, *27*, 34.
[88] Z. Cui, Y. Han, Q. Huang, J. Dong, Y. Zhu, *Nanoscale* **2018**, *10*, 6806.
[89] S. Savagatrup, E. Chan, S. M. Renteria-Garcia, A. D. Printz, A. V. Zaretski, T. F. O'Connor, D. Rodriquez, E. Valle, D. J. Lipomi, *Adv. Funct. Mater.* **2015**, *25*, 427.

[90] J. A. Fan, W.-H. Yeo, Y. Su, Y. Hattori, W. Lee, S.-Y. Jung, Y. Zhang, Z. Liu, H. Cheng, L. Falgout, *Nat. Commun.* **2014**, *5*, 3266.
[91] S. K. Ameri, M. Kim, I. A. Kuang, W. K. Perera, M. Alshiekh, H. Jeong, U. Topcu, D. Akinwande, N. Lu, *npj 2D Mater. Appl.* **2018**, *2*, 19.
[92] J. H. So, J. Thelen, A. Qusba, G. J. Hayes, G. Lazzi, M. D. Dickey, *Adv. Funct. Mater.* **2009**, *19*, 3632.
[93] Y.-L. Park, B.-R. Chen, R. J. Wood, *IEEE Sens. J.* **2012**, *12*, 2711.
[94] M. D. Dickey, *ACS Appl. Mater. Interfaces* **2014**, *6*, 18369.
[95] M. D. Dickey, R. C. Chiechi, R. J. Larsen, E. A. Weiss, D. A. Weitz, G. Whitesides, *Adv. Funct. Mater.* **2008**, *18*, 1097.
[96] C. Pan, K. Kumar, J. Li, E. J. Markvicka, P. R. Herman, C. Majidi, *Adv. Mater.* **2018**, *30*, 1706937.
[97] A. Hirsch, H. O. Michaud, A. P. Gerratt, S. De Mulatier, S. P. Lacour, *Adv. Mater.* **2016**, *28*, 4507.
[98] M. Tavakoli, M. H. Malakooti, H. Paisana, Y. Ohm, D. Green Marques, P. Alhais Lopes, A. P. Piedade, A. T. de Almeida, C. Majidi, *Adv. Mater.* **2018**, *30*, 1801852.
[99] R. K. Kramer, C. Majidi, R. J. Wood, in *2011 IEEE Int. Conf. Robotics Automation*, IEEE, Piscataway, NJ, USA **2011**, pp. 1103–1107.
[100] Y.-L. Park, C. Majidi, R. Kramer, P. Bérard, R. J. Wood, *J. Micromech. Microeng.* **2010**, *20*, 125029.
[101] Y. Mengüç, Y.-L. Park, H. Pei, D. Vogt, P. M. Aubin, E. Winchell, L. Fluke, L. Stirling, R. J. Wood, C. J. Walsh, *Int. J. Rob. Res.* **2014**, *33*, 1748.
[102] P. Won, J. J. Park, T. Lee, I. Ha, S. Han, M. Choi, J. Lee, S. Hong, K.-J. Cho, S. H. Ko, *Nano Lett.* **2019**, *19*, 6087.
[103] K. Yong, S. De, E. Y. Hsieh, J. Leem, N. R. Aluru, S. Nam, *Mater. Today* **2019**, *34*, 58.
[104] C. H. Yang, M. X. Wang, H. Haider, J. H. Yang, J.-Y. Sun, Y. M. Chen, J. Zhou, Z. Suo, *ACS Appl. Mater. Interfaces* **2013**, *5*, 10418.
[105] L. Fillaud, T. Petenzi, J. Pallu, B. Piro, G. Mattana, V. Noel, *Langmuir* **2018**, *34*, 3686.
[106] C. G. Núñez, W. T. Navaraj, E. O. Polat, R. Dahiya, *Adv. Funct. Mater.* **2017**, *27*, 1606287.
[107] L. Shi, T. Zhu, G. Gao, X. Zhang, W. Wei, W. Liu, S. Ding, *Nat. Commun.* **2018**, *9*, 2630.
[108] D. Y. Choi, M. H. Kim, Y. S. Oh, S.-H. Jung, J. H. Jung, H. J. Sung, H. W. Lee, H. M. Lee, *ACS Appl. Mater. Interfaces* **2017**, *9*, 1770.
[109] H. Shi, C. Liu, Q. Jiang, J. Xu, *Adv. Electron. Mater.* **2015**, *1*, 1500017.
[110] J. Lee, P. Lee, H. B. Lee, S. Hong, I. Lee, J. Yeo, S. S. Lee, T. S. Kim, D. Lee, S. H. Ko, *Adv. Funct. Mater.* **2013**, *23*, 4171.
[111] J. P. Thomas, L. Zhao, D. McGillivray, K. T. Leung, *J. Mater. Chem. A* **2014**, *2*, 2383.
[112] D. J. Lipomi, M. Vosgueritchian, B. C. Tee, S. L. Hellstrom, J. A. Lee, C. H. Fox, Z. Bao, *Nat. Nanotechnol.* **2011**, *6*, 788.
[113] J. Jung, H. Lee, I. Ha, H. Cho, K. K. Kim, J. Kwon, P. Won, S. Hong, S. H. Ko, *ACS Appl. Mater. Interfaces* **2017**, *9*, 44609.
[114] C.-J. Lee, K. H. Park, C. J. Han, M. S. Oh, B. You, Y.-S. Kim, J.-W. Kim, *Sci. Rep.* **2017**, *7*, 7959.
[115] X. Wang, Y. Zhang, X. Zhang, Z. Huo, X. Li, M. Que, Z. Peng, H. Wang, C. Pan, *Adv. Mater.* **2018**, *30*, 1706738.
[116] R. Wang, W. Xu, W. Shen, X. Shi, J. Huang, W. Song, *Inorg. Chem. Front.* **2019**, *6*, 3119.
[117] B. W. An, S. Heo, S. Ji, F. Bien, J.-U. Park, *Nat. Commun.* **2018**, *9*, 2458.
[118] A. Miyamoto, S. Lee, N. F. Cooray, S. Lee, M. Mori, N. Matsuhisa, H. Jin, L. Yoda, T. Yokota, A. Itoh, *Nat. Nanotechnol.* **2017**, *12*, 907.
[119] S. Lee, D. Sasaki, D. Kim, M. Mori, T. Yokota, H. Lee, S. Park, K. Fukuda, M. Sekino, K. Matsuura, *Nat. Nanotechnol.* **2019**, *14*, 156.
[120] H. S. Jo, S. An, J.-G. Lee, H. G. Park, S. S. Al-Deyab, A. L. Yarin, S. S. Yoon, *NPG Asia Mater.* **2017**, *9*, e347.
[121] H. Lee, S. Hong, J. Lee, Y. D. Suh, J. Kwon, H. Moon, H. Kim, J. Yeo, S. H. Ko, *ACS Appl. Mater. Interfaces* **2016**, *8*, 15449.
[122] G. Zhu, P.-g. Ren, J. Wang, Q. Duan, F. Ren, W. Xia, D.-X. Yan, *ACS Appl. Mater. Interfaces* **2020**, *12.17*, 19988.
[123] C. Xu, M. Colorado Escobar, A. A. Gorodetsky, *Adv. Mater.* **2020**, *32*, 1905717.
[124] G. Wang, X. Chen, S. Liu, C. Wong, S. Chu, *ACS Nano* **2016**, *10*, 1788.
[125] S. Shang, Q. Zhang, H. Wang, Y. Li, *J. Colloid Interface Sci.* **2016**, *483*, 11.
[126] H. Kim, M. Seo, J. W. Kim, D. K. Kwon, S. E. Choi, J. W. Kim, J. M. Myoung, *Adv. Funct. Mater.* **2019**, *29*, 1901061.
[127] M. Moirangthem, A. P. Schenning, *ACS Appl. Mater. Interfaces* **2018**, *10*, 4168.
[128] G. H. Lee, T. M. Choi, B. Kim, S. H. Han, J. M. Lee, S.-H. Kim, *ACS Nano* **2017**, *11*, 11350.
[129] G. Lee, G. Y. Bae, J. H. Son, S. Lee, S. W. Kim, D. Kim, S. G. Lee, K. Cho, *Adv. Sci.* **2020**, *7*, 2001184.
[130] H. Kim, H. Lee, I. Ha, J. Jung, P. Won, H. Cho, J. Yeo, S. Hong, S. Han, J. Kwon, *Adv. Funct. Mater.* **2018**, *28*, 1801847.
[131] H. Yuk, S. Lin, C. Ma, M. Takaffoli, N. X. Fang, X. Zhao, *Nat. Commun.* **2017**, *8*, 14230.
[132] B. B. Kang, H. Choi, H. Lee, K.-J. Cho, *Soft Rob.* **2019**, *6*, 214.
[133] P. Polygerinos, Z. Wang, K. C. Galloway, R. J. Wood, C. J. Walsh, *Rob. Auton. Syst.* **2015**, *73*, 135.
[134] N. Kellaris, V. G. Venkata, G. M. Smith, S. K. Mitchell, C. Keplinger, *Sci. Rob.* **2018**, *3*, eaar3276.
[135] R. L. Truby, M. Wehner, A. K. Grosskopf, D. M. Vogt, S. G. Uzel, R. J. Wood, J. A. Lewis, *Adv. Mater.* **2018**, *30*, 1706383.
[136] S. Y. Kim, Y. Choo, R. A. Bilodeau, M. C. Yuen, G. Kaufman, D. S. Shah, C. O. Osuji, R. Kramer-Bottiglio, *Sci. Rob.* **2020**, *5*, eaay3604.
[137] M. Wehner, R. L. Truby, D. J. Fitzgerald, B. Mosadegh, G. M. Whitesides, J. A. Lewis, R. J. Wood, *Nature* **2016**, *536*, 451.
[138] S.-J. Park, M. Gazzola, K. S. Park, S. Park, V. Di Santo, E. L. Blevins, J. U. Lind, P. H. Campbell, S. Dauth, A. K. Capulli, *Science* **2016**, *353*, 158.
[139] C. A. Aubin, S. Choudhury, R. Jerch, L. A. Archer, J. H. Pikul, R. F. Shepherd, *Nature* **2019**, *571*, 51.
[140] S. Han, T. Kim, D. Kim, Y.-L. Park, S. Jo, *IEEE Rob. Autom. Lett.* **2018**, *3*, 873.
[141] T. G. Thuruthel, B. Shih, C. Laschi, M. T. Tolley, *Sci. Rob.* **2019**, *4*, eaav1488.
[142] I. Van Meerbeek, C. De Sa, R. Shepherd, *Sci. Rob.* **2018**, *3*, eaau2489.
[143] S. Sundaram, P. Kellnhofer, Y. Li, J. Y. Zhu, A. Torralba, W. Matusik, *Nature* **2019**, *569*, 698.
[144] J. Kim, M. Lee, H. J. Shim, R. Ghaffari, H. R. Cho, D. Son, Y. H. Jung, M. Soh, C. Choi, S. Jung, K. Chu, D. Jeon, S. T. Lee, J. H. Kim, S. H. Choi, T. Hyeon, D. H. Kim, *Nat. Commun.* **2014**, *5*, 5747.
[145] J. Zhong, Y. Ma, Y. Song, Q. Zhong, Y. Chu, I. Karakurt, D. B. Bogy, L. Lin, *ACS Nano* **2019**, *13*, 7107.
[146] Y. Jin, Y. Lin, A. Kiani, I. D. Joshipura, M. Ge, M. D. Dickey, *Nat. Commun.* **2019**, *10*, 4187.
[147] H. Fan, K. Li, Q. Li, C. Hou, Q. Zhang, Y. Li, W. Jin, H. Wang, *J. Mater. Chem. C* **2017**, *5*, 9778.
[148] S. Taccola, F. Greco, E. Sinibaldi, A. Mondini, B. Mazzolai, V. Mattoli, *Adv. Mater.* **2015**, *27*, 1668.
[149] J.-H. C. Guofa Cai, Y. Liu, Y. Jiang, P. S. Lee, *Sci. Adv.* **2019**, *5*, eaaw7956.
[150] Y. Han, T. Bai, Y. Liu, X. Zhai, W. Liu, *Macromol. Rapid Commun.* **2012**, *33*, 225.
[151] B.-U. Hwang, A. Zabeeb, T. Q. Trung, L. Wen, J. D. Lee, Y.-I. Choi, H.-B. Lee, J. H. Kim, J. G. Han, N.-E. Lee, *NPG Asia Mater.* **2019**, *11*, 23.
[152] B. You, C. J. Han, Y. Kim, B.-K. Ju, J.-W. Kim, *J. Mater. Chem. A* **2016**, *4*, 10435.
[153] Y. Bao, Y. Han, L. Yang, N. Li, J. Luo, W. Qu, R. Chen, A. K. Y. Jen, T. Li, H. Chen, *Adv. Funct. Mater.* **2019**, *29*, 1806383.
[154] E. Karshalev, R. Kumar, I. Jeerapan, R. Castillo, I. Campos, J. Wang, *Chem. Mater.* **2018**, *30*, 1593.
[155] C. Yu, Y. Li, X. Zhang, X. Huang, V. Malyarchuk, S. Wang, Y. Shi, L. Gao, Y. Su, Y. Zhang, *Proc. Natl. Acad. Sci. USA* **2014**, *111*, 12998.

Phillip Won received his B.S. degree in material science and engineering at the University of Illinois at Urbana Champaign in 2014. He is currently a Ph.D. student at Seoul National University working in the Applied Nano and Thermal Science Lab under the supervision of Professor Seung Hwan Ko. His research focus is on the fabrication of flexible and stretchable electrodes using nanomaterials.

Kyun Kyu Kim received his B.S. degree in the Department of Mechanical Engineering at Korea University in 2014. He is currently a Ph.D. student at Seoul National University working in the Applied Nano and Thermal Science Lab under the supervision of Professor Seung Hwan Ko. His research focus is on augmented wearable electronics based on nanomaterials and laser fabrication combined with machine intelligence.

Hyeonseok Kim received his B.S. degree in the Department of Mechanical Engineering at the Yonsei University in 2013. He is currently a Ph.D. student at Seoul National University working with the Applied Nano and Thermal Science Lab under the supervision of Professor Seung Hwan Ko. His research focus is on the biomimetic soft robotics based on polymers and nanomaterials with a laser fabrication process.

Seung Hwan Ko is a professor in Applied Nano and Thermal Science (ANTS) Lab, Mechanical Engineering Department, Seoul National University, Korea. Before joining Seoul National University, he had been a faculty at Korean Advanced Institute of Science and Technology (KAIST), Korea since 2009. He received his Ph.D. degree in mechanical engineering from University of California, Berkeley in 2006. He worked as a postdoc at UC Berkeley until 2009. His current research interests are stretchable/flexible electronics, transparent electronics, soft robotics, wearable electronics, laser assisted nano/microfabrication and crack assisted nanomanufacturing.